

IMPACT OF CENTERLINE NO-SLIP ON VORTEX TUBE PERFORMANCE

by

PARIKSHIT. B. PARDESHI

A thesis submitted to the

Graduate School–New Brunswick

Rutgers, The State University of New Jersey

In partial fulfillment of the requirements

For the degree of

Master of Science

Graduate Program in Mechanical and Aerospace Engineering

Written under the direction of

Dr. Michael. R. Muller

And approved by

New Brunswick, New Jersey

JANUARY, 2016

ABSTRACT OF THE THESIS

IMPACT OF CENTERLINE NO-SLIP ON VORTEX TUBE PERFORMANCE

By PARIKSHIT. B. PARDESHI

Thesis Director:

DR. MICHAEL. R. MULLER

The Ranque-Hilsch vortex tube or simply the vortex tube is a device that separates a high pressure gas into a low pressure hot stream and a low pressure cold stream simultaneously without the need for a power supply. Although this device is largely applied for cooling, especially spot cooling of electronic controls, machining operations and such, there has been certain interest in exploring its phase separation ability.

This thesis presents results of an innovative method that is aimed towards improving the phase separation and condensate collection application of the vortex tube. In this study a centerline no-slip condition is introduced in the vortex tube by suspending different inserts (rods and tubes) through it. The effects on the cooling capacity of the vortex tube along with the effects on inlet, cold and hot mass flow rates are observed. The experimental results indicate that even though the inserts negatively impact the refrigeration effect at higher cold fractions, for lower cold ratios the method works satisfactorily. There is a definite increase in cold mass flow rate due to centerline no-slip with corresponding decrease in hot mass flow rates. The reasons for this phenomenon are explored in the thesis. It was also concluded that as the outer diameter of the insert

increases, the refrigeration effect decreases. A stainless steel rod of outer diameter 1/8” turned out to be the optimum insert for the current study.

This study also aims at locating the centerline axial stagnation point by analyzing the temperature profile along the centerline of the vortex tube.

ACKNOWLEDGEMENT

I would like to take this opportunity to thank my advisor, Dr. Michael R. Muller, without whom this thesis wouldn't have been possible. I am grateful to him for his continuous guidance, support, patience and encouragement which got me through my most frustrating moments during the research. I would like to thank my thesis committee members, Dr. Javier Diez-Garias and Dr. Jerry Shan, for their participation. I would like to extend my gratitude towards Mr. John Petrowski for his invaluable suggestions and guidance through my research. I am grateful to Mr. Samuel Ramrajkar who helped me learn, understand and apply the concepts of electrical engineering. I would like to thank PhD student Mr. Chris Deppe for his patience and help finding things around the labs. Further, I would like to mention my dear friends, Ms. Mary Gettings and Ms. Noopur Gosavi, who had taken up the responsibility of keeping me strong throughout my stay at Rutgers. Lastly, my special thanks goes to my family back in India who has sacrificed a lot to fulfill my dream of pursuing masters in USA.

TABLE OF CONTENTS

Abstract	ii
Acknowledgement	iv
List of Tables	viii
List of Illustrations	ix
Nomenclature	xi
1. Introduction	1
1.1 Objectives.....	1
1.2 Motivation.....	1
1.3 History and Overview of the VT.....	2
1.4 Structure of the VT.....	3
1.4.1 Types of VTs.....	3
1.4.2 Cross-section of a VT.....	3
1.5 Working of a VT.....	5
1.6 Literature Review.....	6
1.6.1 Thermo-physical Parameters.....	7
1.6.2 Geometrical Parameters.....	8
1.6.3 Energy Separation.....	8
1.6.4 Stagnation Point.....	10
1.6.5 Phase Separation.....	10
1.6.6 Summary of Literature Review.....	12
2. Experimental Setup and Non-Dimensionalization	13
2.1 Setup.....	13

2.2 Non-Dimensionalization of Thermo-physical Parameters.....	15
2.2.1 Refrigeration Capacity (Q).....	15
2.2.2 Mass Flow Rates.....	16
2.2.3 Frequency and amplitude of vibration.....	16
3. Experimentation, Results and Discussion.....	17
3.1 Centerline no-slip condition using fishing lines and wires.....	17
3.1.1 Nature of vibrations induced in the wire.....	18
3.2 Centerline no-slip condition using tubes and rods.....	20
3.3 Error Measurement.....	30
4. Conclusion and Future Work.....	31
4.1 Conclusion.....	31
4.2 Future Work.....	32
5. Appendix.....	33
5.1 Pre-setup.....	33
5.1.1 Accommodations for inserts and leakage prevention.....	33
5.1.2 Measurement of resistance output of thermistor.....	35
5.1.3 Suspension of the thermistor through the tube.....	36
5.2 Experimental Procedures.....	37
5.2.1 Experiment on vibrations.....	37
5.2.2 Measurement of impact of centerline no-slip condition on VT.....	38
5.2.3 Experiment to measure the temperature profile along the centerline...	39
5.3 Instrumentation.....	40
6. References.....	44

6.1 References for figures.....	44
6.2 References for literature review.....	44

LIST OF TABLES

Table 1.	Instrumentation.....	40
----------	----------------------	----

LIST OF ILLUSTRATIONS

Figure 1.	(a) Counterflow VT and (b) Uniflow VT (NIT Rourkela).....	3
Figure 2.	Cross-section of a VT.....	3
Figure 3.	Generator (Scienceforums).....	4
Figure 4.	Working of a VT (ITW Vortec).....	5
Figure 5.	Process Flow Diagram.....	13
Figure 6.	Experimental setup to measure the impact of centerline no-slip on VT.	14
Figure 7.	Vibrational modes of the wire induced by vortices in the VT.....	18
Figure 8.	Frequency and amplitude of vibrations in the wire.....	19
Figure 9.	Effect on Cooling Efficiency for inserts vs Cold Fraction, (a) $P_i/P_a = 1.34$, (b) $P_i/P_a = 2.02$, (c) $P_i/P_a = 2.7$	21
Figure 10.	Effect on Cold and Hot mass flow rates for 3/16” rod.....	23
Figure 11.	Location of stagnation point in the VT.....	24
Figure 12.	Location of Stagnation Point at 15 Psi (a) Choi and Riu [24] based on wall temperature (b) Chang-Hyun Sohn et al.[23] based on surface tracing method (c) Based on Cooling Efficiency.....	25
Figure 13.	Effect of centerline no-slip on the position of stagnation point.....	26
Figure 14.	Effect of centerline no-slip condition on the flow structure in the VT...	26
Figure 15.	Secondary flow in the VT as shown by Ahlborn et al [18].....	27
Figure 16.	Change in cold mass flow rate and change in dT vs change in cooling capacity for 3/16”rod.....	28
Figure 17.	Effect of centerline no-slip condition on the inlet mass ratio at various inlet pressure ratios, (a) $C_f = 0.3$, (b) $C_f = 0.5$, (c) $C_f = 0.7$	29
Figure 18.	Histogram representing distribution of actual energy conserved around the ideal energy conservation.....	30
Figure 19.	Leakage prevention through the hot exhaust valve.....	33
Figure 20.	Leakage prevention through the air hoses.....	34
Figure 21.	Voltage divider circuit to measure resistance output from thermistors..	35

Figure 22.	Suspension of thermistor through a SS tube.....	36
Figure 23.	Measurement of vibrations induced in the wire.....	37
Figure 24.	Setup for measuring centerline temperature profile.....	38
Figure 25.	Thermistor.....	40
Figure 26.	Pressure Gauge.....	40
Figure 27.	Vortex Tube.....	40
Figure 28.	Velmex Bislid Linear Stage.....	41
Figure 29.	Precision Turbine Flow meter with signal conditioner.....	41
Figure 30.	Signal Amplifier.....	42
Figure 31.	Stroboscope.....	42
Figure 32.	Pressure Transducer.....	43
Figure 33.	Data Acquisition Card.....	43

NOMENCLATURE

M_i	: mass flow rate at the inlet of the VT.
M_c & M_h	: mass flow rate at the cold end and the hot end, respectively.
C_f & H_f	: Cold fraction (M_c / M_i) and Hot fraction (M_h / M_i), respectively.
T	: static temperature.
dT	: differential temperature.
P	: static pressure.
c_p, c_v	: specific heat capacities at constant pressure and volume.
k	: ratio of specific heats.
W	: specific work of the compressor.
Q	: refrigeration capacity of the VT.
R	: gas constant for air.
D	: inside diameter of the VT.
F	: forced frequency.
F_n	: natural frequency.
A	: amplitude of vibration.

CHAPTER 1

INTRODUCTION

In this chapter, the objective and the motivation behind this research are discussed. Further, VT is introduced with simple notes on its history, basic working and previous researches conducted on it.

1.1 Objectives

The objectives of this research work are as follows:

- Studying the application of centerline no-slip boundary condition for improvement of phase separation capabilities of the VT and analyzing its impact on performance of the VT, specifically on the refrigeration capacity, mass flow rates and cold ratio
- Obtain an optimum insert to be used to create the centerline no-slip boundary condition.
- Determine the location of the centerline axial stagnation point by analyzing the centerline temperature profile in the VT.

1.2 Motivation

Traditional methods of phase separation in the hydrocarbon industry like drying, gas dehydration and condensate recovery by the means of turboexpanders, phase separators and glycol, have known to be high energy consuming processes with a heavy negative impact on the environment [31]. Further, these processes require regular maintenance and chemical replacements causing the operation cost to increase. The need for an efficient, less-polluting technology with relatively lower operational cost has generated an interest in the VT technology for the industries and

researchers alike. This thesis aims at facilitating an innovative way to use a VT for phase separation and condensate collection and studies its impact on the VT performance.

Further, researchers like Pourmahmoud et al. [14] showed that most part of the energy separation occurs before the stagnation point. Consequently, they concluded that the position of the stagnation point is an important criterion in improving the energy separation and optimizing the length and other geometrical parameters of the VT. This thesis also aims at locating the axial stagnation point by analyzing the temperature profile along the centerline of the VT.

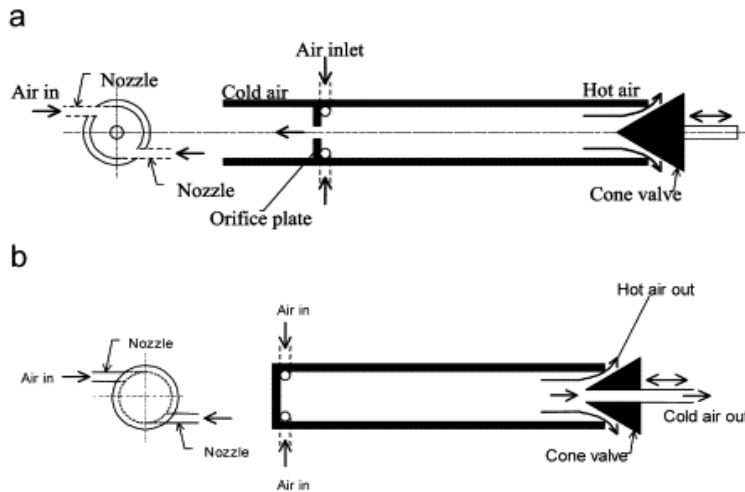
1.3 History and Overview of the VT

The VT was invented in 1930s by a French physicist Georges Ranque [1] and was further improved by German physicist Rudolf Hilsch [2], hence the name Ranque-Hilsch. It was first developed for industrial use in 1960s by Vortec [32]. Since then it has been used in a wide variety of applications like cooling machining operations, soldered parts, cooling of electronic components etc. The advantages of using a VT are that it neither requires any energy input, except for the compressor, nor does it have any moving parts therefore, providing a clean, long-term maintenance-free operation. Other advantages include low cost, reliability, compactness and working without refrigerants. One interesting feature of the VT is the varied range of cooling capacity that can be controlled by supply pressure and a conical exhaust valve at the hot end.

1.4 Structure of the VT

1.4.1 Types of VTs

There are two types of VTs – Uniflow and Counterflow (Figure 1).



As seen from the figure, a counterflow VT has the cold and hot streams coming out from the opposite ends whereas in the uniflow VT the streams come out from the same end.

Figure 1. (a) Counterflow VT and (b) Uniflow VT.(NIT Rourkela)

It was observed by T. Cockerill [34] that the cooling capacity of the uniflow tube is lower and so counterflow VT is used widely.

1.4.2 Cross-section of a VT

A general cross-section of a counterflow VT is shown in Figure 2.

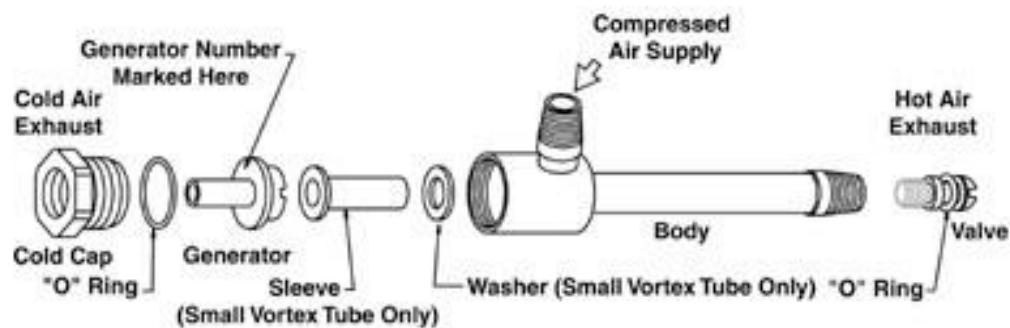


Figure 2. Cross-section of a Counterflow VT. (Exair)

As seen from Figure 2, a vortex tube has following main parts –

- **Generator:** It is situated right below the supply pipe and it forces the gas to



enter the body in a smooth tangential motion in order to form a vortex. It is interchangeable and it also regulates the volume of compressed gas so that flow rate and temperature ranges can be controlled.

Figure 3. Generator (Scienceforums)

- **Body:** The vortices travel along the body towards the exits.
- **Hot Exhaust Adjustment Valve:** The position of this valve determines the amount the air to be let through the hot exhaust. It acts as the main differential temperature controller.
- **Sleeve:** It provides a passage for the cold inner vortex to pass to the cold end exhaust.
- **Cold Cap:** It holds the generator in place and also acts as the cold end exhaust.

1.5 Working of a VT

This thesis is based on experiments conducted using dry air as it is easily available and most widely used.

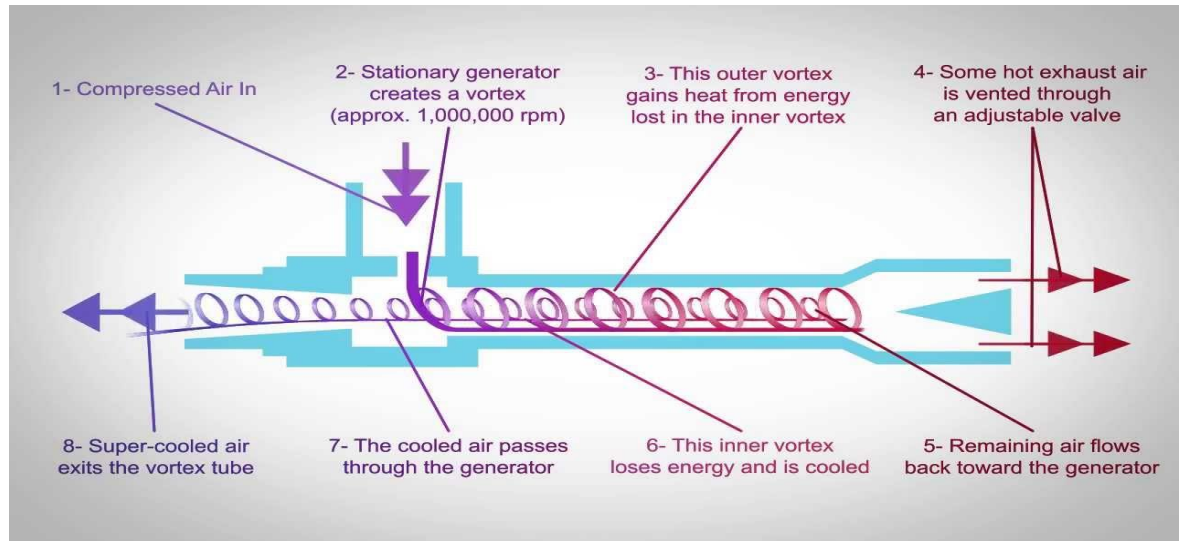


Figure 4. Working of a VT. (ITW Vortec)

Referring to Figure 4, working of the VT can be broken down into following 8 steps:

- 1- **Compressed Air Supply:** Compressed air supplied from an external source enters the VT through the inlet.
- 2- **Generation of vortices:** The stationary generator makes the air to enter in a smooth tangential manner thus creating an outer vortex. At the stagnation point the air from outer vortex forms a concentric inner vortex which moves towards the cold exhaust.
- 3- **Heating up of outer vortex:** As the outer vortex moves along the length of the body, it heats up by taking the energy from the inner vortex and due to friction with the wall.

- 4- **Hot air exhaust:** The outer hot vortex exits the tube from the hot end side. The amount of hot air that is allowed to go out can be controlled by the position of the adjustment valve which is tapered.
- 5- **Return of the remaining air:** The remaining air returns along the length of the body as the inner smaller vortex.
- 6- **Energy exchange between vortices:** Along its way towards the cold exhaust, the inner vortex loses energy thus getting cooler. At the same time, this energy is absorbed by the outer vortex thus increasing its temperature. There are many theories that seek to explain the phenomenon of energy separation but none of them has been conclusive. These theories are explained in the literature review section of this thesis.
- 7- **Inner vortex passing through the generator:** The inner vortex passes through the generator and a sleeve which lead it towards the cold exhaust.
- 8- **Cold air exhaust:** The inner cooled vortex is let out from the cold exhaust and this can be directly used for cooling and refrigeration.

1.6 Literature Review

There has been a vast amount of research on VTs since Rudolf Hilsch [2] first improved upon Georges Ranque's [1] original work, with over 250 articles being published. A major part of this research is dedicated in understanding and improving the temperature separation phenomenon in the VT. Not all of the reviewed literature is directly connected to the current study but it helps to understand the effects on VT better.

The research work on VT can be broadly classified into three categories:

- Experimental and theoretical effect of change in thermo-physical parameters like inlet gas, temperature, pressure, etc.
- Experimental and theoretical effect of change in geometrical parameters like length, generator etc.
- Energy models to understand the energy separation phenomenon in the VT.

1.6.1 Thermo-physical Parameters

Many researchers studied the effect of change in thermo-physical parameters on the VT performance both experimentally and by means of numerical simulation. Kargaran [3], and Orhan and Muzaffar [8] separately performed experimental studies by varying the inlet pressure. It was concluded that the cold and hot temperature differences increase dramatically with increase in the inlet pressure. Rajarshi Kar et al. [7] conducted experimental studies and Pourmahmoud et al. [4] performed numerical simulations of the effect of inlet gas temperature. Both researches concluded that increase in the inlet gas temperature leads to an increase in both hot and cold temperature differences. Further, Pourmahmoud recommended that since for high inlet temperatures the gas leaving out of cold exit is too hot for cooling, the hot exit gas can be used for industrialized processes which might need heating or pre-heating.

There has been a lot of research performed on the effect on VT performance for various supply fluids. Pourmahmoud et al. [9] used NO₂, CO₂, O₂, N₂ and air to study the effect on the performance of the VT using a CFD model. Their results show that NO₂ works the best in terms of both cooling and heating capacities. Initial study on the separation of mixtures in the VT was performed by Linderstorm-Lang [5]. Marshall [6] used the Linderstrom-Lang VT to conclude there is a critical inlet Reynolds number for

maximum separation by this device. Gas mixtures used in these experiments were CO₂ + air, N₂ + O₂ etc.

1.6.2 Geometrical Parameters

Many researchers conducted studies on optimization of geometrical parameters in order to achieve best VT performance. Investigations done by Nimbalkar and Muller [10] concluded that the effect of cold end orifice diameter is negligible for cold fractions less than 60%. Pourmahmoud [11] performed CFD simulations to measure the effect of change in length on the position of the stagnation point and hence the performance of the VT. Their study concluded that optimum length of the vortex tube depends upon operating parameters and other geometrical factors such as inlet pressure, flow rate, the diameter of the vortex tube etc. It further stated that increasing the length to diameter ratio (L/D) beyond 9.3 has no effect on the performance of the VT. Kirmaci [12] used the Taguchi methods, a set of statistical methods used to improve quality of manufactured goods, to optimize the number of nozzles of the VT. These experiments were carried out under different conditions of inlet pressure, nozzle number and fluid type. Wu et al. [13] designed a new nozzle with equal gradient of Mach number and a new intake flow passage of nozzles with equal flow velocity to reduce the energy loss due to friction. This study concluded the new design to be better performing than the current designs of VT manufacturers.

1.6.3 Energy Separation

Since the time Ranque [1] developed the VT, a lot of theories have been investigated to understand the phenomenon of energy separation in the VT. Ranque [1] himself attributed the energy separation to adiabatic expansion in the central region and

adiabatic compression in the peripheral region. Hilsch [2] used similar ideas to explain the energy separation but introduced internal friction between the vortices which caused the entire fluid to undergo solid body rotation. Further, Xue and Arjomandi [21] also considered adiabatic expansion as a main factor for temperature separation in the VT. Shultz-Grunow [15] believed that the energy separation is due to turbulent heat transfer in the VT. Ahlborn et al. [16] hypothesized that the cooling and heating is linked to the increase or decrease in the kinetic energy of the fluid. They state that the hot component entering the VT slows down as it exits through the larger hole and this loss of kinetic energy leads to gain in the temperature whereas, the inner vortex accelerates through the small hole on the cold exit thus increasing its kinetic energy and decreasing the temperature. Kurosaka [17] attributed the energy separation to the fundamental functions of orderly disturbances and found a relationship between acoustic resonance frequencies and the forced vortex motion frequency. The study proposed that the energy separation is due to the damping of the acoustic streaming along the axis of the tube towards the hot exhaust. Stephan et al. [22] proposed the formation of Görtler vortices on the inside wall of the VT that drive the fluid motion. Görtler vortex is formed in a boundary layer flow near a concave wall when the centrifugal action creates a pressure variation (instability) across the boundary layer. Thus, the energy separation is due to the disturbance motion of the Görtler vortex. Fulton [24] hypothesized that the energy separation is due to the formation of free vortices near the wall and forced vortices at the center of the VT.

Many studies were performed to understand the flow structure in the VT. Ahlborn and Groves [18] made a breakthrough by experimentally observing the presence of secondary flow in the vortex tube using a pitot tube. It was determined that the return

flow at the center of the tube is larger than the cold mass flow exiting the VT. Therefore, there must be a secondary circulation that moves the fluid from the back flow core to the outer regions. This was further confirmed by Nimbalkar [10]. Liew et al. [19] measured velocities inside the VT by means of Laser Doppler Anemometry and concluded the turbulence to be isotropic in the core of the VT. Saidi and Yazdi [20] applied exergy destruction model to explain the phenomenon of energy separation. This approach included losses due to heat transfer and pressure drop.

1.6.4 Stagnation Point

It is well-known that stagnation point plays an important role in energy separation in the VT. Therefore, many experimental as well as theoretical studies have been conducted in order to locate the stagnation point. Chang-Hyun et al. [23] performed surface tracing method by injecting dye on the VT wall and visualizing it. The study indicated the location of stagnation point based on the abrupt change of trajectory on the VT wall. It concluded that the stagnation point moves toward the vortex generator with increase in cold flow ratio and inlet pressure which is same as the results obtained by Nimbalkar [25]. Choi and Riu [24] stated that stagnation point lies where the outer wall temperature of the VT is the highest. Further, this theory was confirmed by Pourmahmoud et al. [14] by using CFD. Although there has been a lot of research on the stagnation point, its actual location still remains elusive.

1.6.5 Phase separation

Even though there have been a lot of investigations on the ability of VT to separate gas mixtures, the application of VT for phase separation remains largely untouched. Saidi and Valipour [26] conducted experiments to check the effect of

moisture content on the VT performance. They injected water into the inlet flow and measured cold and hot flow temperatures. The study concluded that the cold temperature difference and efficiency decrease by increasing the moisture content of the air. Khodorkov et al. [27] investigated the application of VT for cleaning, and drying gases and separating mixtures. Stanescu et al. [28] discussed the potential for increasing the air moisture removal by recovering wasted pressure energy. Saha et al. [29] discovered that the number of nozzles does not affect the droplet separation in the VT. Further, it was concluded that for water vapor, the cold side of the VT becomes oversaturated for cold-fraction of 10-50%, therefore implying the application of VT for phase separation. Liew et al. [30] numerically studied the droplet behavior in a VT. The studied showed that negative radial flow near the inlet imparted radial drag on the droplets thus moving them towards the axis of the VT. Further, when the centrifugal force overcomes the radial drag force, the droplets move towards the wall. The study showed that the condensation occurs in the first few centimeters of the vortex tube on the cold side. It was also noted that adding a contaminant increases the phase separation efficiency of the VT as it helps form larger droplets.

Apart from research in labs, various field studies have been performed in Germany where VT was used as a phase separator. Gröner [31] of RWE Energy reported more than 5 years of successful operation of the use of VT for gas dehydration. The study concluded that VT was an economic, efficient and faster option against conventional dehydration and reduced the negative impact on the environment.

1.6.6 Summary of Literature Review

- Condensation in the VT occurs near the cold end side. Further, the fluid becomes oversaturated for cold fractions of 10% - 50%.
- There is evident advantage of using VT for drying and gas dehydration processes in hydrocarbon industry.
- The cooling efficiency of VT drops due to the presence of moisture.
- Even though a heavy research has been performed to locate the stagnation point, it still remains elusive.

It can be concluded that there is a need to explore and improve the phase separating abilities of a VT in order to provide a clean, maintenance free and efficient option, mainly in hydrocarbon industry. Further, a new approach is needed to understand and pinpoint the location of stagnation point in the VT

CHAPTER 2

EXPERIMENTAL SETUP AND NON-DIMENSIONALIZATION

In Chapter 2, the experimental setup and process flow are explained. Further, non-dimensionalization of the thermo-physical parameters is explained in detail.

2.1 Setup

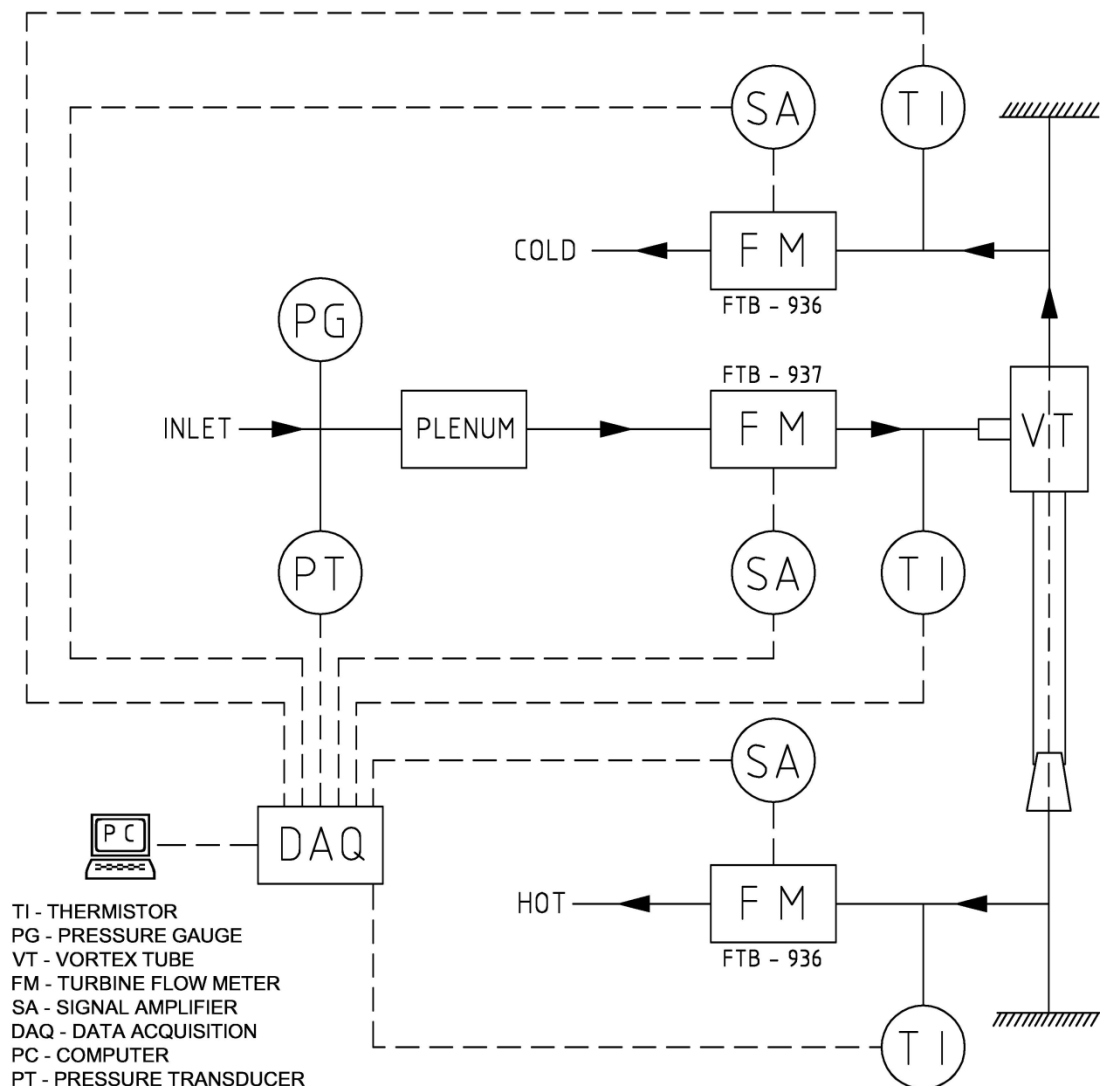


Figure 5. Process flow diagram

Referring to Figure 5, compressed dry air is let into the plenum chamber after being set to the desired value by using a pressure reduction valve. The pressure is measured

using a pressure transducer. From the plenum chamber, the air is then directed to the inlet of the VT where it is split into a hot and a cold stream. These streams then individually exhaust to the atmosphere. The VT is mounted on a linear stage in order to move it vertically to measure the temperature profile along the centerline. A metallic insert (SS tubes and rods) is inserted into the VT (to create centerline no-slip boundary condition) and held between two fixtures. As seen from the figure, the hot stream had to be directed downwards because of space constraints between the larger OD of the VT and the linear stage. Turbine flow meters (with signal amplifiers) and thermistors are introduced in the inlet, cold and hot lines each to measure the mass flow rates and temperatures respectively. Electrical signals from the instruments are directed to a data acquisition system and measured using DasyLab software. The VT used for this study had $L/D = 14.7$. Detailed specifications of the instruments are presented in the Appendix section.

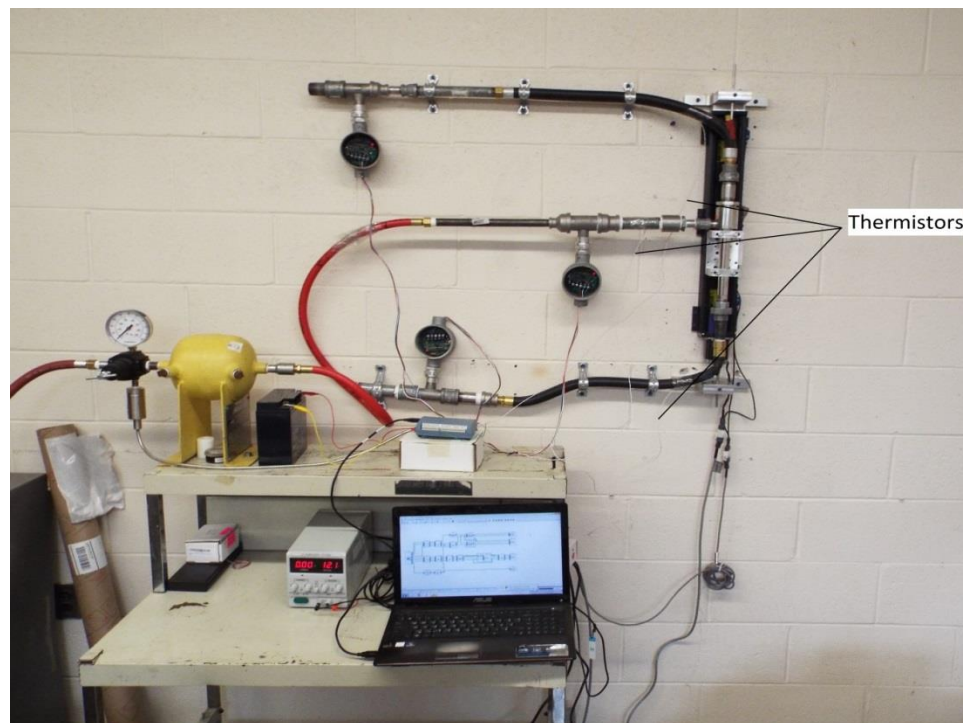


Figure 6. Experimental setup to measure the impact of centerline no-slip on VT

2.2 Non-Dimensionalization of Thermo-physical parameters.

In order to ensure the repeatability of the experiments, parameters like temperature, pressure, mass flow rate, frequency of vibration and length of the vortex tube had to be non-dimensionalized. Each of the parameters is considered individually as follows.

2.2.1 Refrigeration Capacity (Q)

Throughout this thesis, the term ‘performance’ of the VT is synonymous with the cooling effect. Most of the researchers didn’t non-dimensionalize differential temperatures ($T_i - T_c$, $T_h - T_i$ & $T_h - T_c$) or used inlet temperature (T_i) in order to do so. The problem in using T_i as the base parameter, as correctly noted by S. Nimbalkar [10], is that if the compressor is located at a remote location, then T_i does not change with inlet pressure (P_i). Since, the experiments are carried out at different P_i s and since the differential temperatures are functions of P_i , it would be incorrect to use T_i as the base parameter for non-dimensionalization. On the other hand, if the compressor was located in-house, using T_i as the base parameter could be justified as it would change with P_i . Therefore, it was decided to non-dimensionalize refrigeration capacity. Refrigeration Capacity per unit mass can be defined as,

$$Q = cp \times (T_i - T_c) \text{ J/kg} \dots\dots\dots 1$$

where cp is the specific heat of air at constant pressure.

Specific work done by the compressor, to compress the air to the required pressure, is as follows:

$$W = \frac{k}{k-1} \times R \times T_a \times \left\{ \left(\frac{P_i}{P_a} \right)^{\frac{k-1}{k}} - 1 \right\} \text{ J/Kg} \dots\dots\dots 2$$

where $k = 1.4$, is the ratio of specific heats for air, $R = 287 \text{ J/kg K}$, is the gas constant for air.

Therefore, the cooling efficiency is,

$$E = Cf \times \frac{Q}{W} \times 100 \dots\dots\dots 3$$

where Cf is the cold ratio (M_c / M_i)

2.2.2 Mass Flow Rates

The cold and hot mass flow rates have already being non-dimensionalized as cold fraction and hot fraction respectively.

$$Cf = M_c / M_i \ \& \ Hf = M_h / M_i \dots\dots\dots 4$$

2.2.3 Frequency and amplitude of vibration

The forced frequency of vibration can be non-dimensionalized with respect to the natural frequency of the insert. The natural frequency of the string can be calculated using the following equation:

$$F_n = \frac{1}{2L} \sqrt{\frac{T}{\rho}} \dots\dots\dots 5$$

where T is the tension in the string, L is the length of the string and ρ the mass per unit length for of the string.

Further, amplitude of vibration depends upon the orifice diameter and therefore is non-dimensionalized using the orifice diameter.

CHAPTER 3

EXPERIMENTATION, RESULTS AND DISCUSSION

This chapter deals with details of the experiments, the presentation of the results and discussion to obtain suitable conclusions. The detailed experimental procedures are presented in the Appendix. In order to create a centerline no-slip condition in the VT, an insert (metallic rods and tubes) is introduced into the VT. This disrupts the fluid dynamics along the centerline and a boundary layer is created around the insert where the fluid velocity is zero. It is expected that the liquid will condense and slide down along the surface of the insert and can be collected outside the VT.

3.1 Centerline no-slip condition using fishing lines and wires.

Before starting the experimentation, it was well understood that the centerline no-slip condition will affect the fluid dynamics in the VT, thus affecting its performance. It was decided that in order to keep the disturbance to the minimal, the insert should be as thin as possible. Therefore, the initial experiments were done using fishing lines and electrical wire. The fishing lines used were of 15lbs, 20lbs 50lbs and 80lbs strength.

For this experiment the cold and hot side piping was dismantled. The inserts were suspended in the VT and held between fixtures. A hole was drilled into the hot exhaust valve, big enough for the insert to pass through it but small enough to prevent heavy air leakage. The VT was then moved vertically in steps along the linear stage. The supply pressure was increased in steps to observe the effects on the insert.

It was observed that the turbulence in the VT induced heavy vibrations in the fishing lines over inlet pressure of 5 Psi, causing those to break. So, it was decided to use commonly available 24 AWG electrical wires.

3.1.1 Nature of vibrations induced in the wire

As noted in Figure 7, the wire was held taut by means of a weight. The VT was moved along vertically and the changes in the nature of vibrations were observed. The VT was moved in small steps and the frequencies and amplitudes of vibrations were measured at each point.

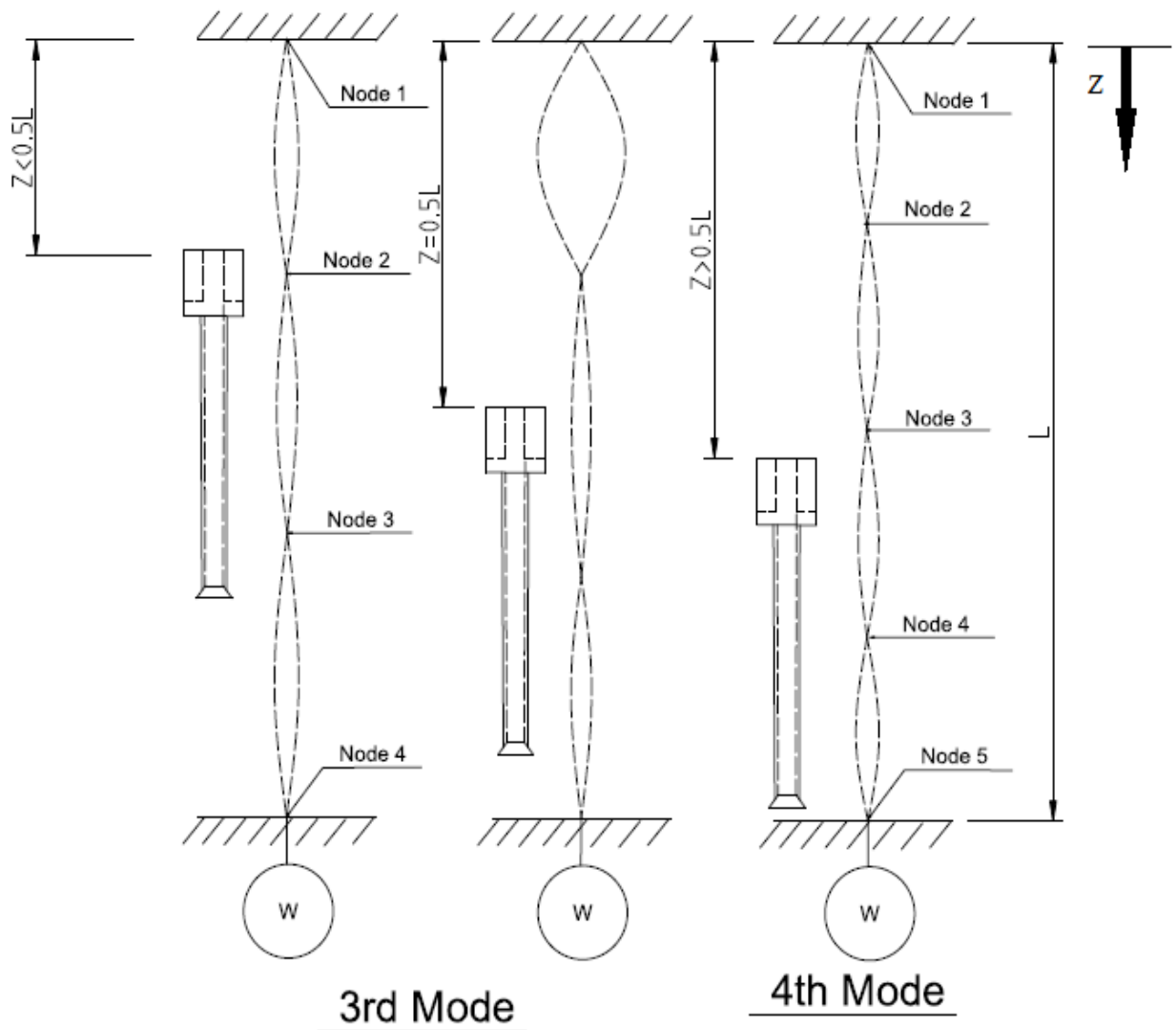


Figure 7. Vibrational modes of the wire induced by vortices in the VT

Using equation 5, the frequency of the wire is calculated as $F_n = 21\text{Hz}$, where $L = 30$ in = length of the wire between the fixtures, $T = 1.25$ lbs = tension in the wire and $\rho = 354\mu$

lb/ft = mass per unit length for 24AWG wire. Figure 8 represents the vibrational frequency and amplitude profiles. Here the amplitude of vibration is non-dimensionalized with respect to the diameter of the orifice.

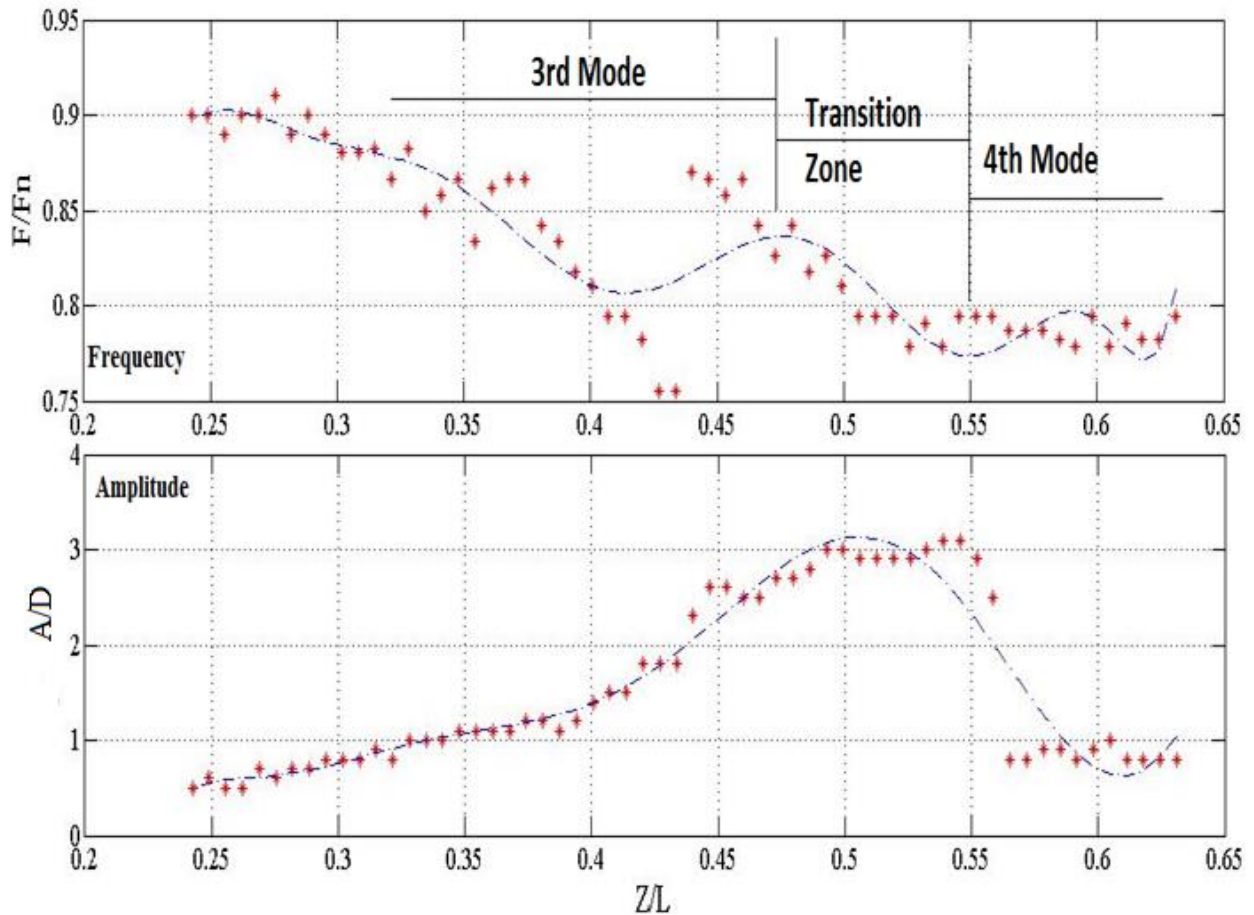


Figure 8. Frequency and amplitude of vibrations in the wire.

As can be seen in Figure 7, the vibrations follow a typical wave formation as in a string and as noted in Figure 8, the observed nature of vibrations can be categorized into three zones depending upon the position of the VT. For $Z < \approx 0.5L$ the wire vibrates in 3rd mode at higher frequency but with lower amplitude, for $\approx 0.45L \leq Z \leq \approx 0.5L$ the wire goes through a transition from 3rd mode to 4th mode of vibration and vibrates with

highest amplitudes and, $Z \geq \approx 0.55L$ where the wire vibrates in 4th mode at lowest frequencies and with lowest amplitudes.

The occurrence of these modes depends upon the position of the VT with respect to the location of nodes and also the length of the wire (L). As can be seen from the figure, for $Z < 0.5L$, two nodes – Node 2 and Node 3 - are inside the VT and the amplitude is curbed by the inner wall of the generator. As the VT moves closer to $Z \approx 0.5L$, Node 2 moves out and therefore, the wire starts vibrating at higher amplitudes. The amplitude keeps increasing until $Z \geq \approx 0.55L$ beyond which the wire starts vibrating in 4th mode. In the 4th mode it is observed that both frequency and amplitude of vibration are the lowest. It is speculated that as the nodes move out of the VT the frequency of vibration is dampened and therefore, it goes on decreasing as Z increases.

It is observed that in order to reduce the vibrations in the string, Z should be kept as large as possible. Further, in order to increase the natural frequency and reduce the amplitude, the load on the wire was increased but the wire snapped for $W > 1.25$ lbs. Another solution would be to hold on to the higher mode by physically pinning the nodes on the wire so that it vibrates with lower amplitude and frequency.

3.2 Centerline no-slip condition using metal tubes and rods

In order to reduce the effect of vibration it was decided to use Stainless Steel rods and tubes as those are sturdier. The tubes and rods were of the outer diameters 1/8", 3/16" and 1/4" each. The performance is not compared with the original factory designed data because a hole is drilled into the hot exhaust valve, thus compromising the design. Therefore, a separate 'no insertion / without insertion with plugged hole' condition was

introduced. Figure 9 represents the effect on cooling efficiency by the inserts versus the cold fractions at different pressure ratios. (WO/I – without insert and with plugged valve).

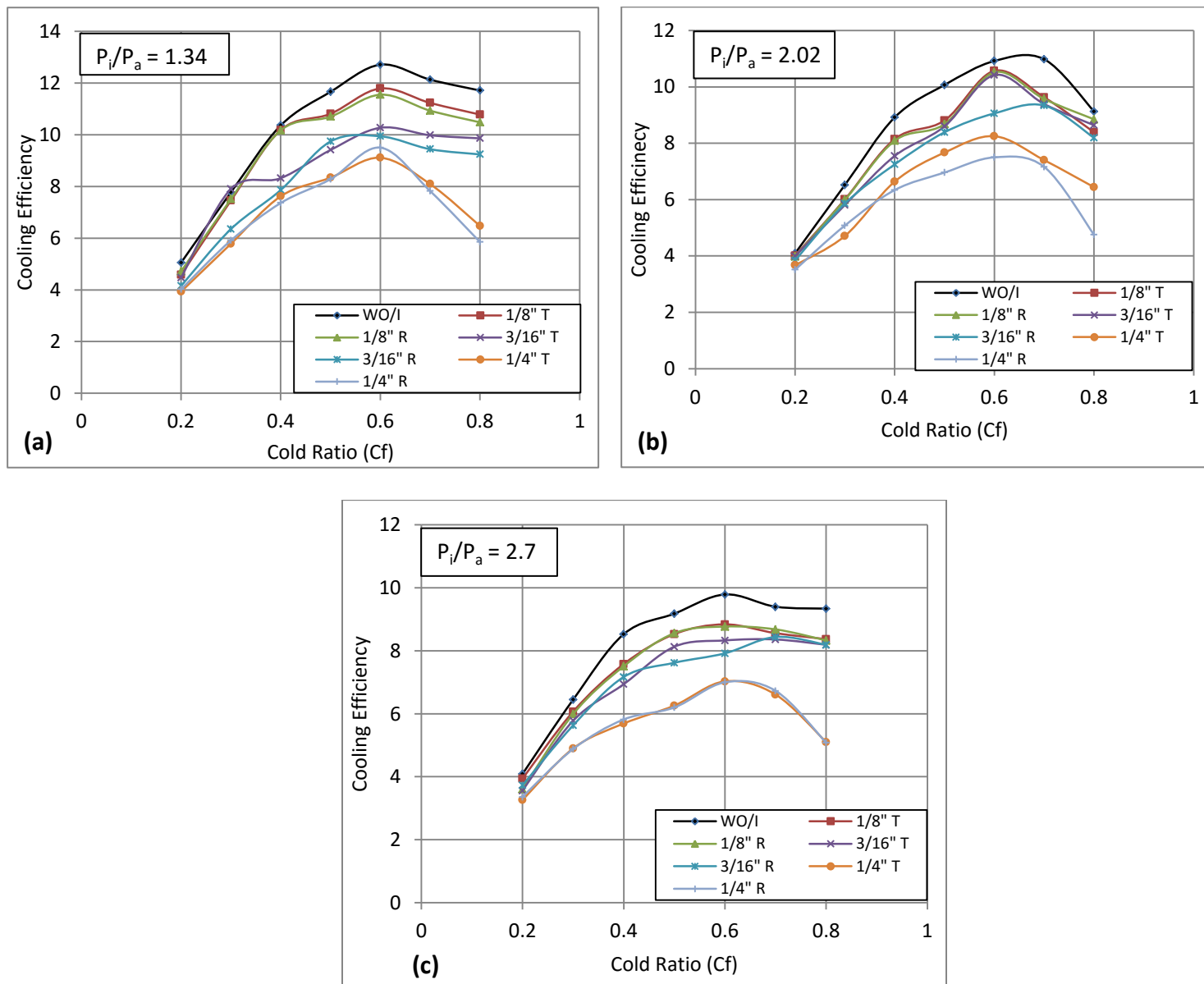


Figure 9. Effect on Cooling Efficiency for inserts vs Cold Fraction,
 (a) $P_i/P_a = 1.34$, (b) $P_i/P_a = 2.02$, (c) $P_i/P_a = 2.7$

From the figure it is observed that smaller the size of the insert lower is the impact on cooling efficiency. It was expected that the inserts would reduce the temperature separation in the VT as those would interfere with the fluid dynamics. It can be said that bigger the insert, higher the interference with the mass flow and hence lower the temperature separation efficiency.

During the experimentation it was observed that the tubes of sizes 1/8" and 3/16" vibrated at pressure ratios >2.0 though with very low frequency and amplitude. The centrifugal forces of the vortices become stronger as the pressure and mass flow rate increase. Therefore, it is speculated that at higher pressures the turbulence becomes strong enough to induce vibrations in the inserts.

At higher supply pressure, 3/16" sized inserts give similar performances as 1/8" inserts. In order to explain this it is hypothesized that as the cold mass flow rate increases, the diameter of the inner vortex increases. For current sized VT, at inlet pressure ratio ≥ 2 this diameter becomes bigger than 3/16" and hence the inserts affect the energy separation to similar extent. Further, the cooling efficiency is highest at cold fraction of 60% – 70%, which is similar to the results obtained by Nimbalkar [25].

The following figure shows the variation in cold and hot end mass flow due to the introduction of 3/16” insert. The scatter plots of the data at different inlet pressures with the corresponding trend lines are shown and are compared with the original without-insert condition.

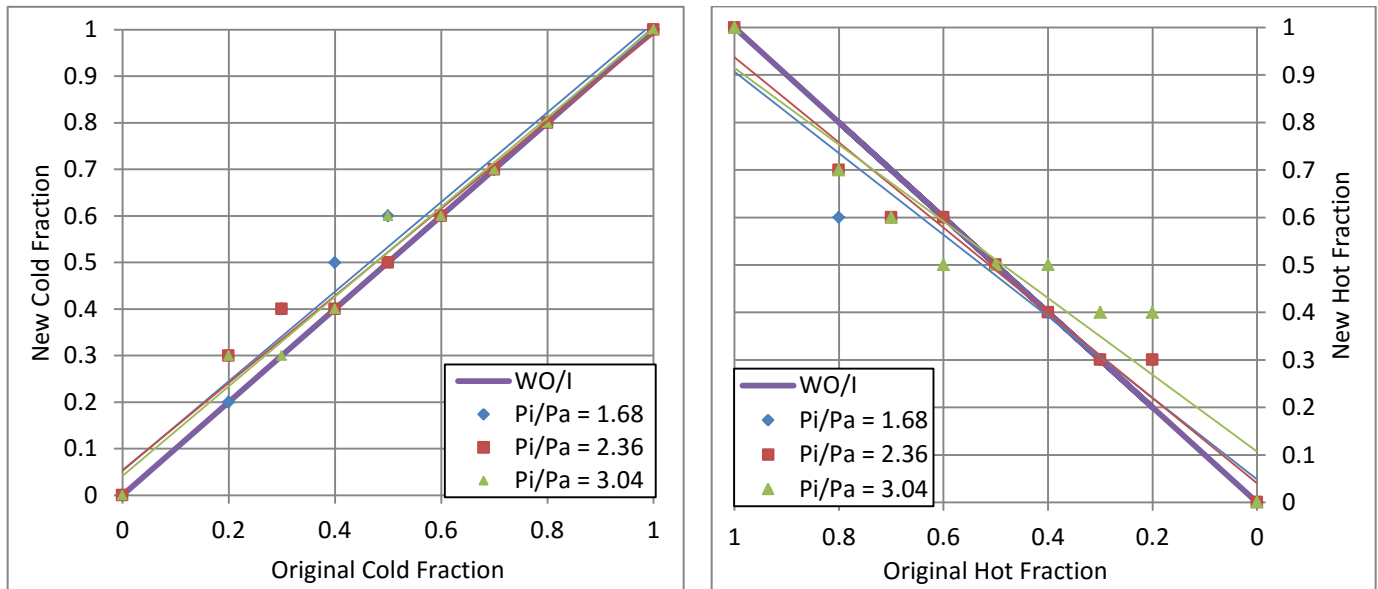


Figure 10. Effect on the Cold and Hot mass flow rates for 3/16” rod

It is found that at any given inlet pressure the cold mass flow rates increase after the introduction of inserts. This is evident particularly at lower cold fractions. Further, this increase in cold mass flow rate diminishes as the cold fraction increases. Similarly, there is a corresponding change in the hot mass flow rate where it decreases at lower cold fractions and increases as the cold fraction increases. For conservation of mass, the sum of cold fraction and hot fraction should be 1 at any given time. It can be observed that this condition is not always fulfilled. This can be attributed to the fluctuations in the supply line and error due to the instrumentation

In order to find the reason for these phenomena, the effects of the insert on the flow structure inside the VT must be understood. Figure 11 shows that the stagnation point is

measured from the center of the inlet nozzle and is non-dimensionalized with respect to the inner diameter of the VT.

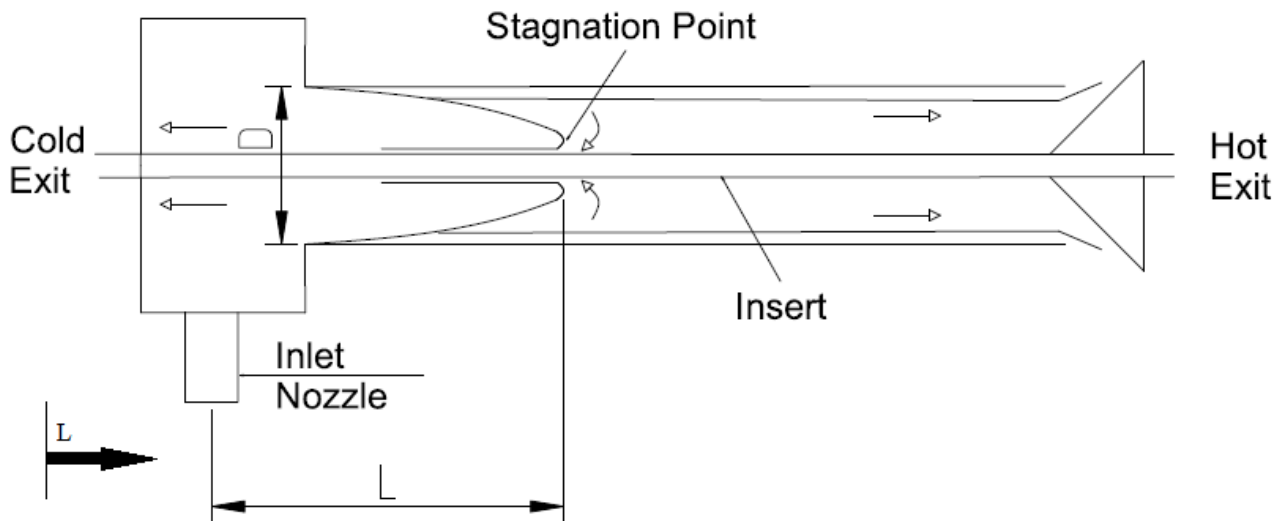


Figure 11. Location of stagnation point in the VT

Figure 12 compares the location of stagnation point at 15 Psi based on the cooling efficiency or centerline temperature separation method with that found by Choi and Riu [24] as highest wall temperature and by Chang Hyung Sohn et al. [23] by surface tracing method. In both of these studies, the location of stagnation point was measured from the center of the inlet nozzle and non-dimensionalized using inner diameter of the VT.

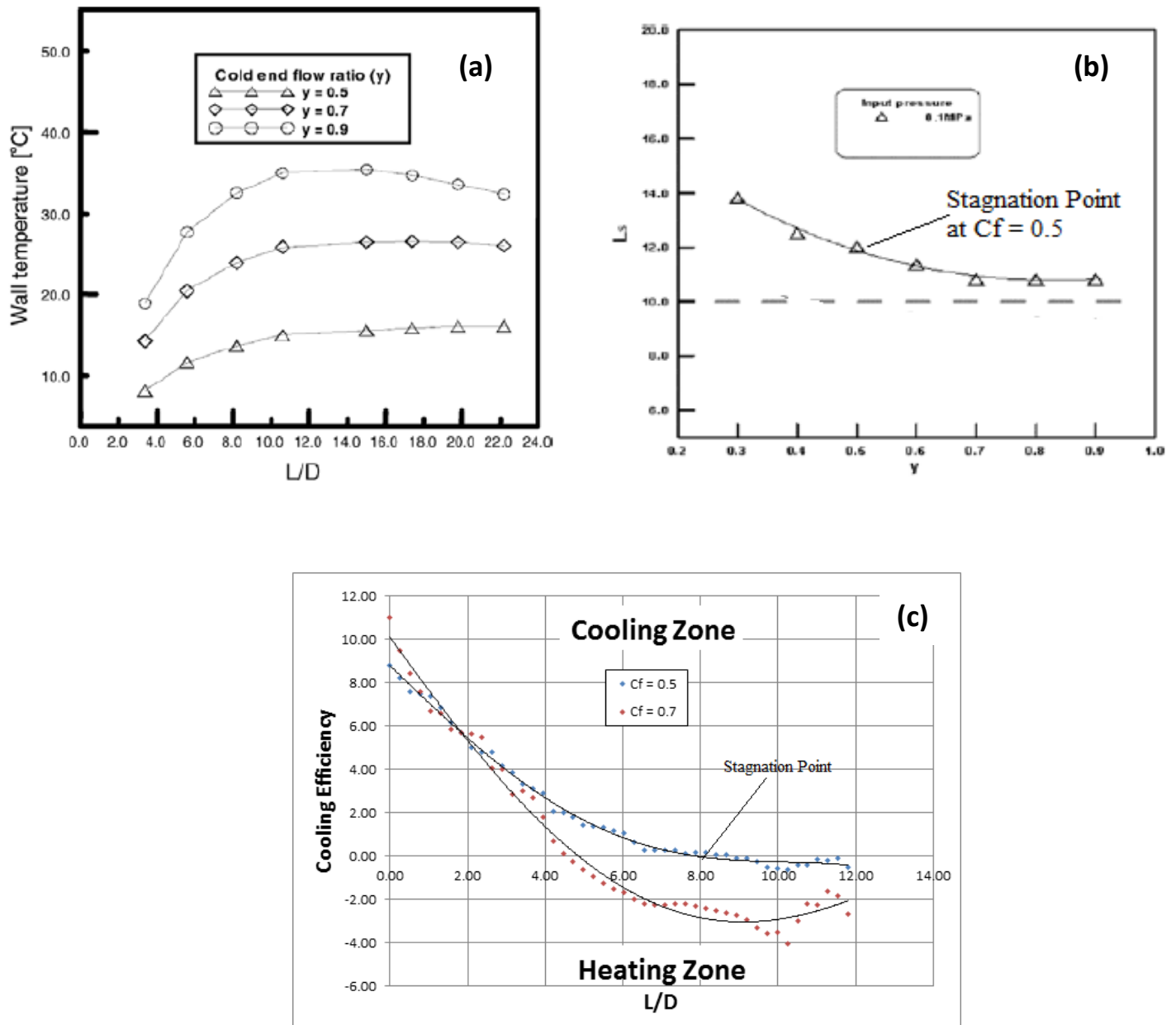


Figure 12. Location of Stagnation Point at 15 Psi (a) Choi and Riu [24] based on wall temperature (b) Chang-Hyun Sohn et al.[23] based on surface tracing method (c) Based on Cooling Efficiency

In VT stagnation point is the point where the energy separation starts therefore; at that point the temperature separation or cooling efficiency is zero. From Figure 12, it is speculated that the stagnation point moves towards the cold exit after the introduction of inserts.

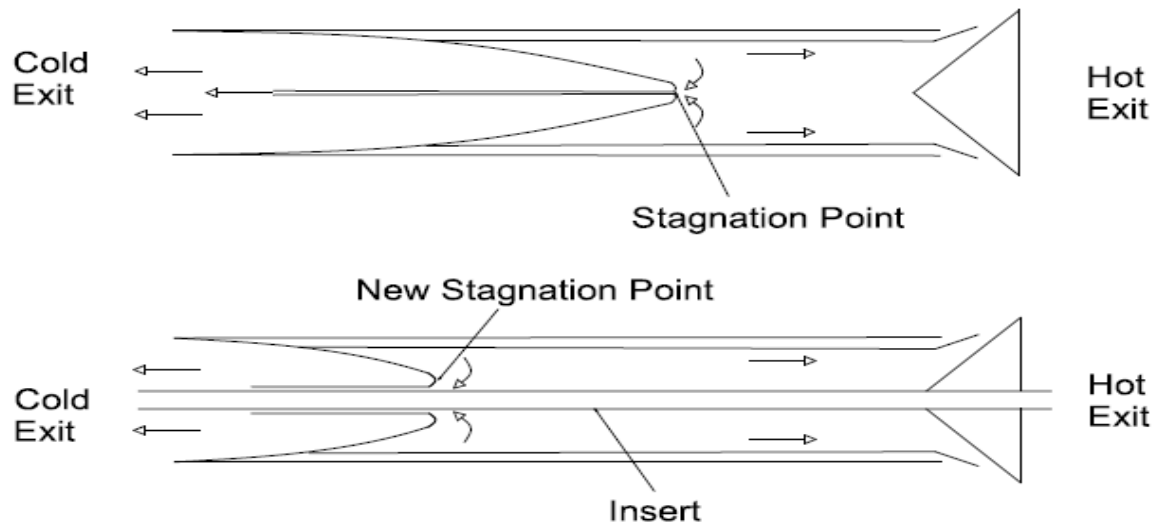


Figure 13. Effect of centerline no-slip condition on the position of stagnation point

It is further speculated that the movement of stagnation point towards the cold exit increases the drag on the mass flowing towards hot exit. As shown in Figure 14, this mass flow, especially that close to the stagnation point, undergoes further pressure and momentum drop while overcoming the drag and tends to move towards the nearest low pressure point i.e. the cold exit.

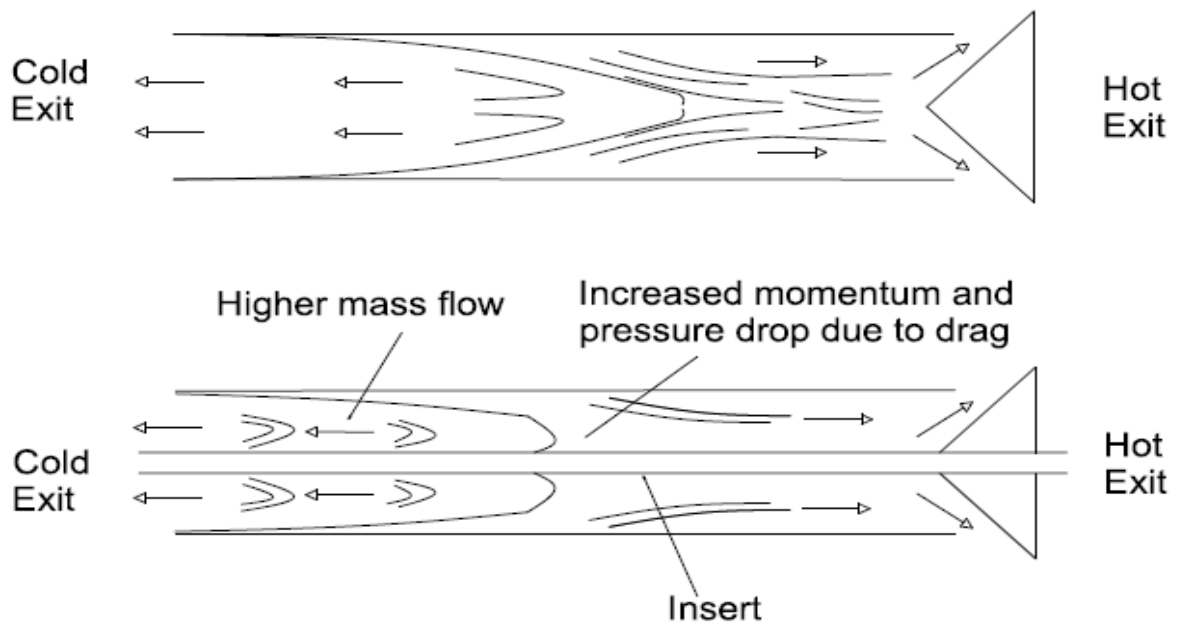


Figure 14. Effect of centerline no-slip condition on the flow structure in the VT

Another probable explanation for the increase in cold mass flow rate can be the reduction of secondary circulation. Ahlborn [18] and Nimbalkar [25] showed the presence of secondary flow in the VT where the mass flow moving towards the cold exit is larger than the mass flow actually coming out of the cold exit. So, the remaining starts moving back as seen in Figure 15.

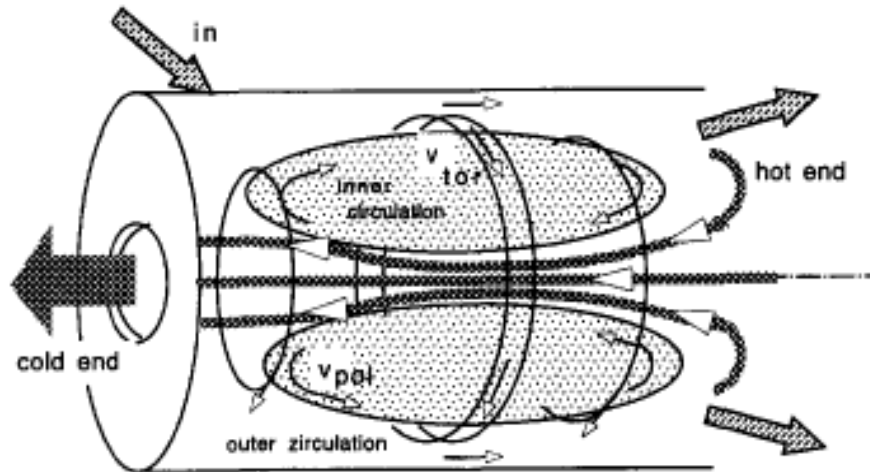


Figure 15. Secondary flow in the VT as shown by Ahlborn et al [18].

It is speculated that the insert cuts into the area of this secondary flow and reduces recirculating mass therefore, leading to higher mass flow towards the cold exit.

In order to characterize the VT as a phase separator reduction in cold temperature is more valuable than the cold mass flow rate. Now, using equation 1, cooling capacity can be defined with as:

$$Q = M_c \times c_p \times dT_c \dots\dots\dots 6$$

where, M_c is cold mass flow rate, c_p is the specific heat of dry air and dT_c is the drop in cold-side temperature. It was observed that even though the centerline no-slip condition increased the cold fraction, it reduced the drop in cold-side temperature. Figure 16 shows that the change in cold temperature differential has a greater effect on the cooling capacity than change in cold mass flow.

Therefore, the cooling capacity drops after adding inserts to the system.

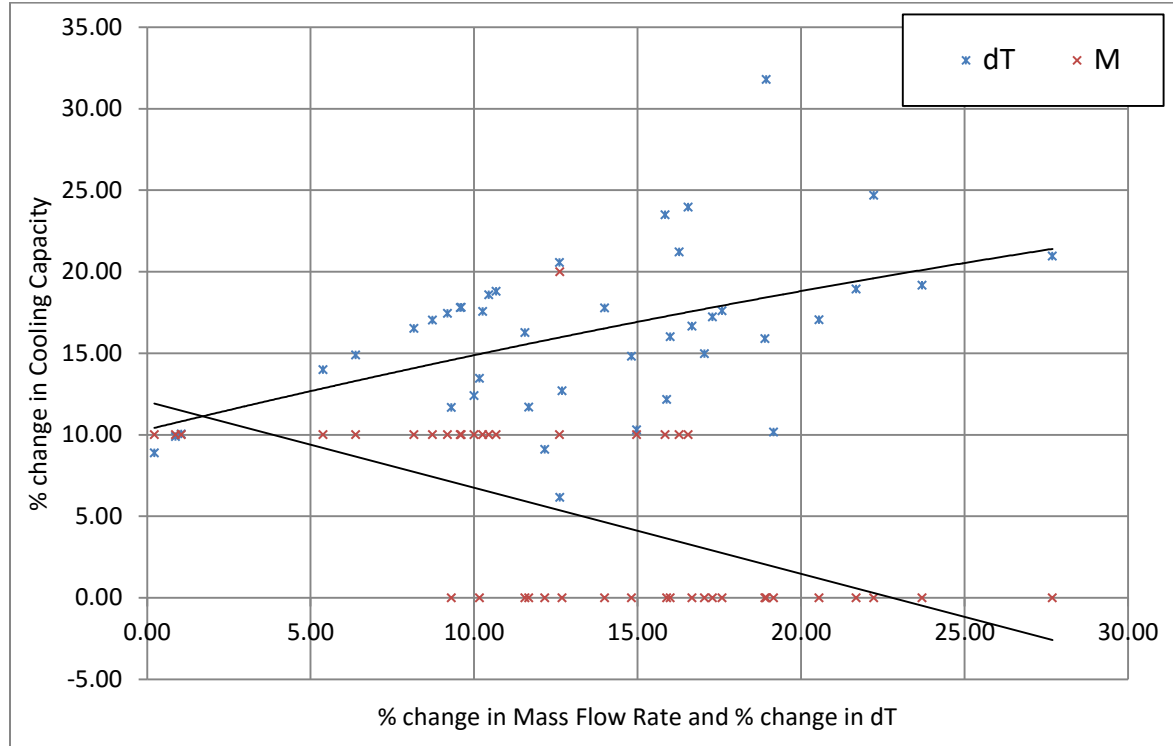


Figure 16. Change in cold mass flow rate and change in dT vs change in cooling capacity for 3/16"rod

In order for the conservation of mass to be satisfied it is important to note any changes in the inlet mass flow rate i.e. the total mass, after the insertions. It was expected that centerline no-slip might increase the back pressure on the supply line therefore changing the inlet mass flow. Figure 17 shows that the inlet mass flow rate ratio is not affected much due to the suspension of the inserts in the VT. The small variations that are observed can be attributed to the fluctuations in the air supply line and to the instrumentation error in measurement.

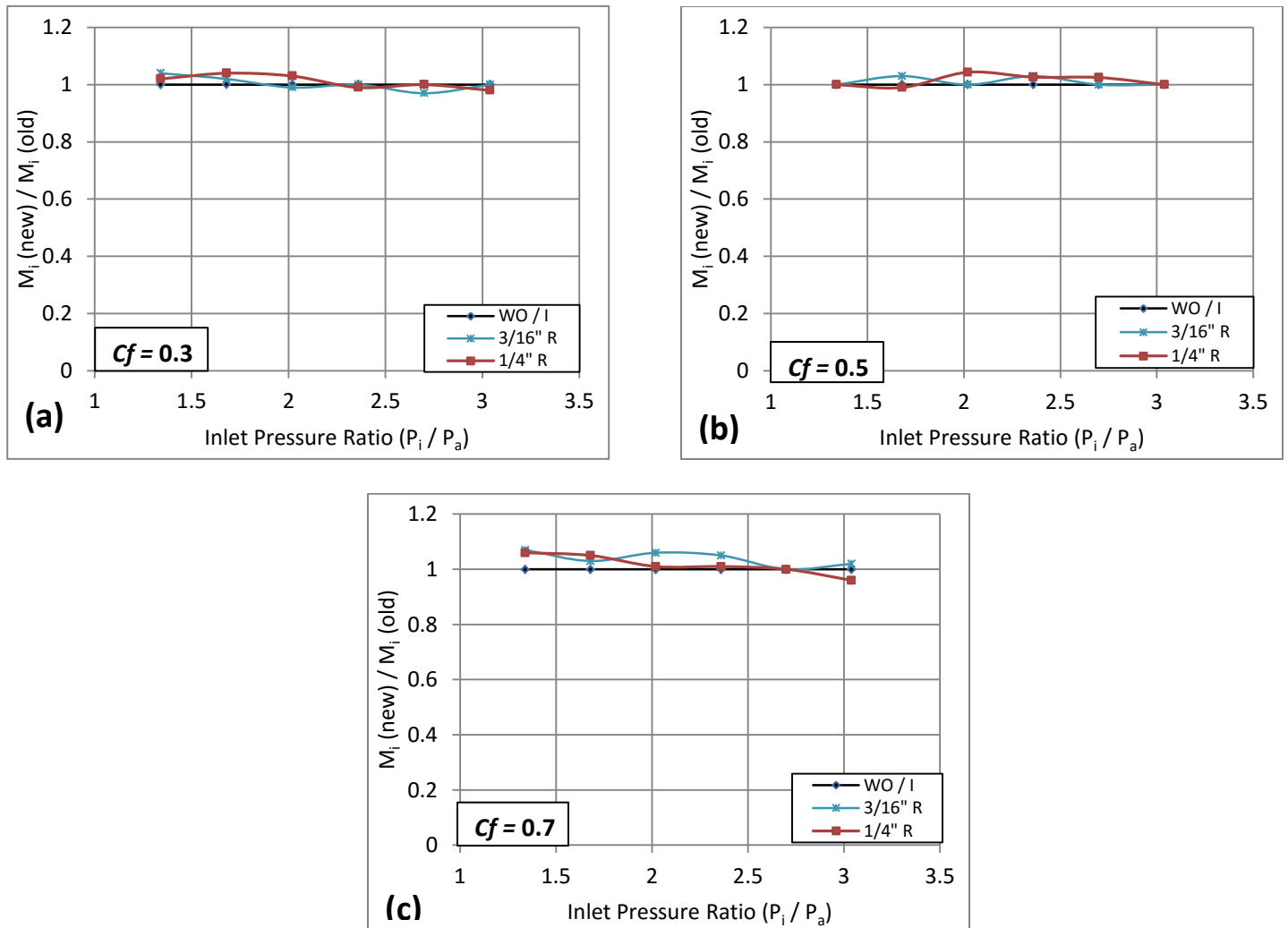


Figure 17. Effect of centerline no-slip condition on the inlet mass ratio at various inlet pressure ratios,
 (a) $C_f = 0.3$, (b) $C_f = 0.5$, (c) $C_f = 0.7$

3.3 Error measurement

The error analysis is done by analyzing conservation of energy in the system. For an ideal system equation 7 must be satisfied.

$$M_i h_i = M_c h_c + M_h h_h \dots\dots\dots 7$$

This kind of analysis gives the cumulative error due to instruments, heat loss due to convection, frictional loss within the fluid and such.

The following histogram shows the distribution of actual energy conserved with respect to the ideal energy conservation for various sets of measurements.

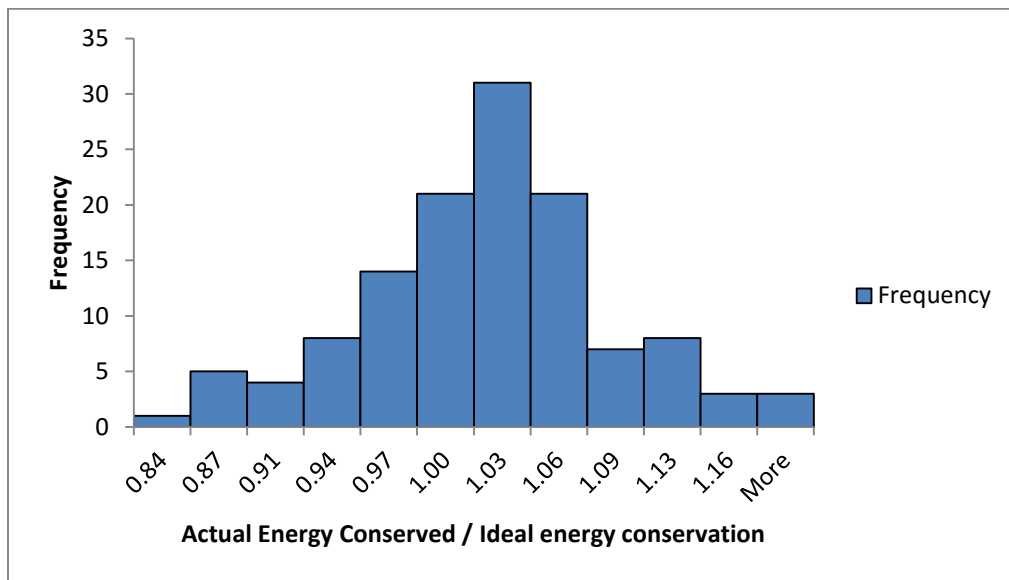


Figure 18. Histogram representing distribution of actual energy conserved around the ideal energy conservation

Relative standard error in measurement can be calculated using the following equation

$$Relative\ Standard\ Error\ (RSE)(\%) = \frac{Std.Deviation / (\sqrt{number\ of\ samples})}{Mean\ of\ the\ sample} \times 100 \dots\dots\dots 8$$

RSE as calculated is $\approx 10\%$.

Therefore, these measurements are 90% accuracy.

CHAPTER 4

CONCLUSION AND FUTURE WORK

This chapter deals with the conclusion of the experiments and presents the scope of work that can be done in the future to improve the results.

4.1 Conclusion

- Curbing the vibrations of the inserts is important as these would tend to splatter the condensate on the wall therefore, defeating the purpose of centerline no-slip boundary condition. The nature of these vibrations depends upon the length and type of the insert and the position of the VT along the length. In order to reduce the frequency and amplitude the VT must be placed such that the inserts vibrate in higher modes. Further, using inserts of higher mass and rigidity diminishes the vibration effect.
- To have least effect on the cooling capacity of the VT, outer diameter of the insert should be kept as low as possible. An optimized size that will have negligible vibration and will least affect the VT performance should be chosen. For this current study, 1/8" rod turned out to be the best option. Further, in order to explain similar performance effects due to 1/8" and 3/16" sized inserts at higher cold fractions, it is hypothesized that the diameter of the inner vortex increases with cold mass flow and at higher cold fractions it becomes bigger than the 3/16" and so the inserts have similar effect on the temperature separation.
- At any given supply pressure the cold mass flow rates increase on introduction of the inserts, especially for lower cold fractions and there is corresponding decrease in the hot mass flow rates. It is speculated that the centerline no-slip moves the

stagnation point towards the cold exit which in-turn increases the drag on the air towards the hot exit. This air, especially closer to stagnation point, loses momentum and pressure energy while overcoming this drag and moves towards the cold exit. Further, the movement of the stagnation point also reduces the temperature separation effect leading to higher cold side temperatures. Another probable reason for the increased cold fraction is that the inserts reduce the effect of recirculation and hence higher mass flows towards cold side.

- Decrease in cold temperature differential due to the inserts has higher effect on the cooling capacity than increase in cold mass flow rate. Therefore, the cooling capacity decreases on introduction of inserts.

4.2 Future Work

There are several areas that can be improved in order to obtain better refrigeration capacities and better condensation and collection.

- Instead of using dry air, humid air or a combination of gas and liquid vapor can be used to check the efficiency of this method.
- The inserts used in this study were of standard commercially available stainless steel sizes. A study can be performed to design an optimum size of the insert that will affect the VT performance the least and improve the efficiency of condensate collection. Further, the inserts can be specially coated to increase the chances of condensate clinging and slipping along the surface.
- The increase in cold mass flow rates should be further explored to pinpoint the reason.

CHAPTER 5

APPENDIX

5.1 Pre-setup

5.1.1 Accommodations for inserts and leakage prevention

In order to accommodate the inserts, holes were drilled in the air hoses and the hot exhaust valve. The threaded hole on the valve could be plugged in order to prevent leakage during “Without Insert” condition. As seen in Figure 19, washers with inner holes of diameter 1/8”, 3/16” and 1/4” were inserted in the valves (one for each insert size) to accommodate the perfect size of the insert and prevent any leakage through the gap.



Figure 19. Leakage prevention through the hot exhaust valve

Further, leakage through the hoses was prevented by means of clogging with clay, as shown in the below figure.



Figure 20. Leakage prevention through the air hoses.

5.1.2 Measurement of resistance output of thermistor

The output of thermistors is resistance (Ohms). The DAQ used in the experimentation was incapable of measuring resistance directly. Hence, the resistance had to be converted into voltage, by means of a voltage divider circuit, before feeding to the DAQ. Referring to Figure 8, the other end of the green wire is connected to the +5V input on DAQ.

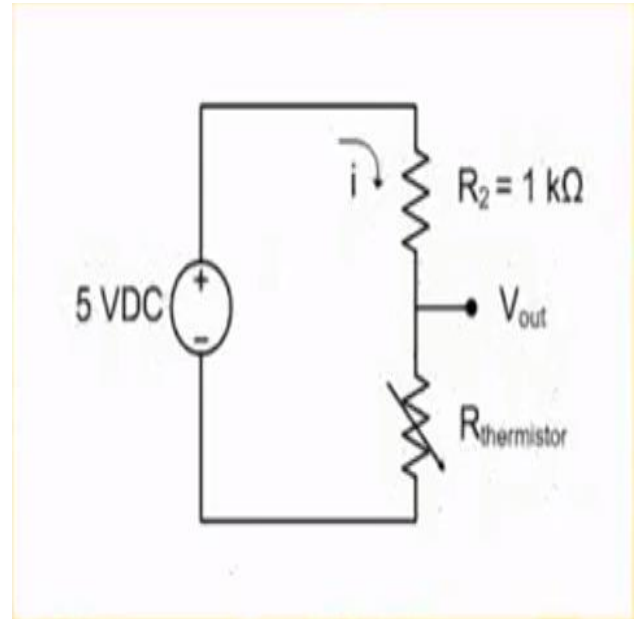
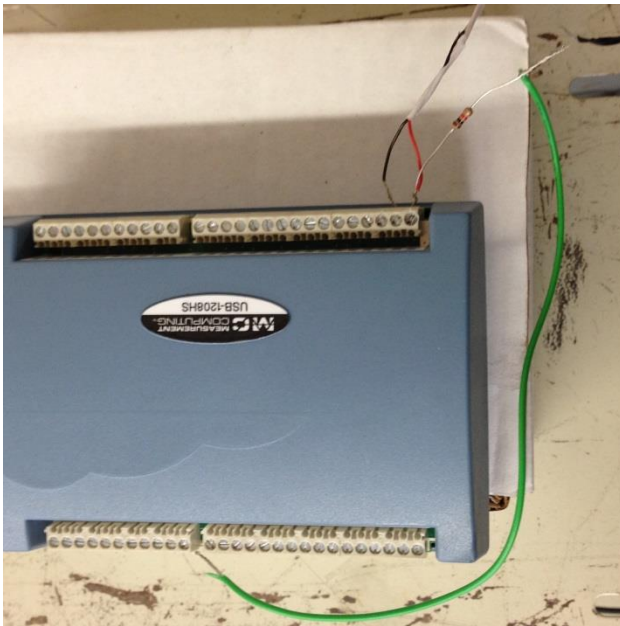


Figure 21. Voltage divider circuit to measure resistance output from thermistors

The measured voltage is reconverted into resistance by using the following equation:

$$R(\text{thermistor}) = \left(\frac{V_{\text{out}}}{5 - V_{\text{out}}} \right) R(2) \dots \dots \dots 7$$

Further, the resistance was converted into temperature by using equation 8

$$T(R) = [A + B \ln \left(\frac{R}{R(25)} \right) + C \ln^2 \left(\frac{R}{R(25)} \right)]^{-1} \dots \dots \dots 8$$

Where,

Resistance of the thermistor at 25 °C = $R(25) = 5000 \Omega$.

Constants provided by Omega Engg

$$A = 1.285 \times 10^{-3}, \quad B = 2.362 \times 10^{-4}, \quad C = 9.285 \times 10^{-8}$$

5.1.3 Suspension of thermistor through the tube

In order to measure the centerline temperature profile, the temperature probe had to be suspended in the VT. Since there was a chance of the probe getting damaged due to the heavy turbulence in the VT, it was suspended through a SS tube. Refer Figure 22.

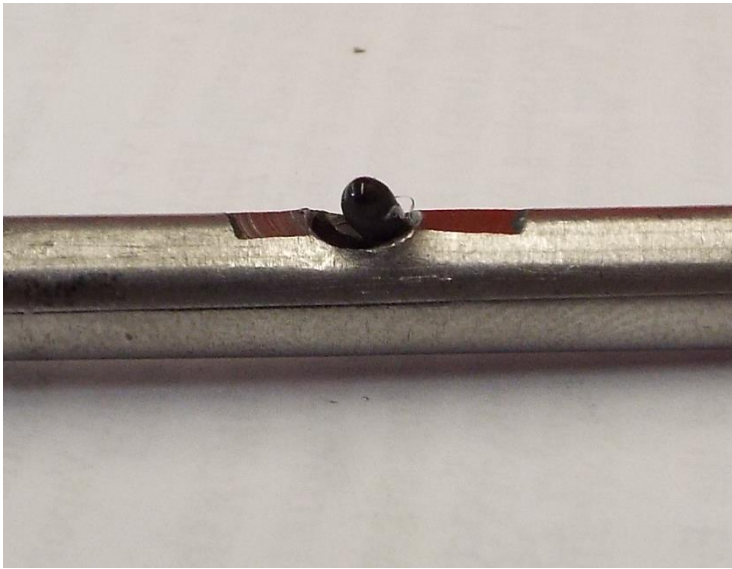


Figure 22. Suspension of thermistor through a SS tube

5.2 Experimental Procedures

5.2.1 Experiment on vibrations

Referring to Figure 23, following steps were followed for the experimentation:

- Step 1.** The wire is suspended through the VT and held taut, by means of a weight, between two fixtures, one each on top and bottom of the linear stage.
- Step 2.** Air is supplied at a set pressure and the frequency and amplitude of the wire are measured.
- Step 3.** The VT is moved by a pre-determined distance along the linear stage and measurements are taken again. This step is repeated till the entire length of the wire between the fixture is covered.
- Step 4.** Supply pressure is increased and Steps 2 & 3 are carried out again.



Figure 23. Measurement of vibrations induced in the wire

5.2.2 Measurement of impact of centerline no-slip condition on VT

The experimental setup is shown in Figure 6..

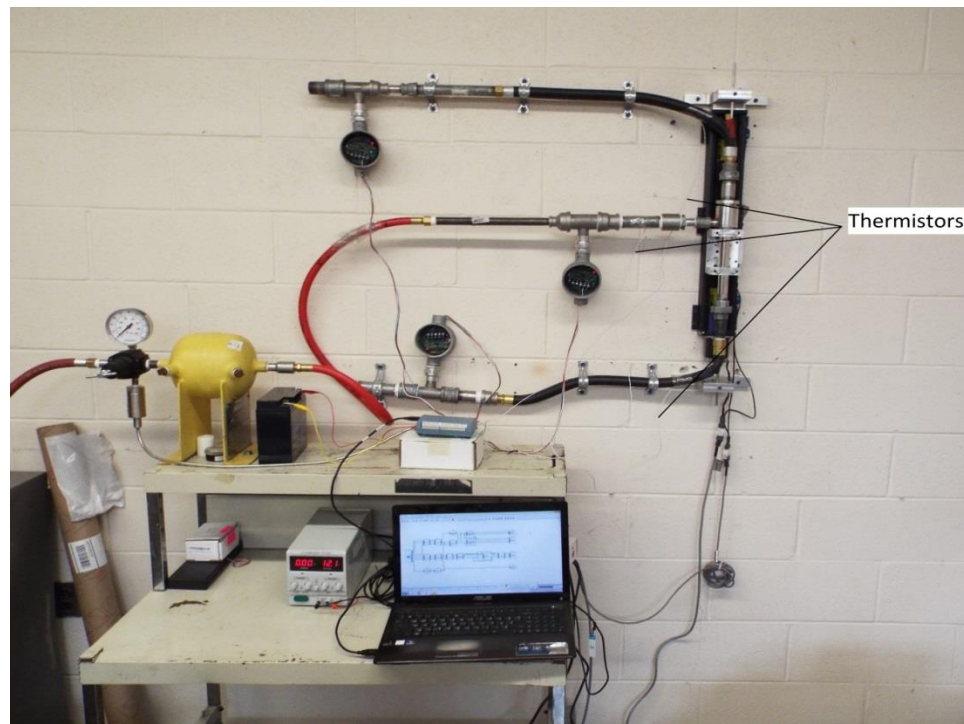


Figure 6. Experimental setup to measure the impact of centerline no-slip on VT

- Step 1.** Air is supplied at a set pressure and the cold fraction is set by measuring the inlet and cold outlet flow rates. The hot gas piping had to be disconnected from the setup in order to control the cold fraction with the hot exhaust valve.
- Step 2.** Hot end piping is reconnected, mass flow rates are measured and the setup is left to achieve thermal stability (approximately 10 minutes).
- Step 3.** Temperatures for inlet and cold and hot gas outlets are measured.
- Step 4.** Tube is inserted through the VT and Steps 2 and 3 are repeated.
- Step 5.** Rod is inserted after removing the tube and Steps 2 and 3 are repeated.
- Step 6.** Steps 1 – 5 are repeated for a new cold fraction.
- Step 7.** Steps 1 – 6 are repeated for higher supply pressure.
- Step 8.** All of the above steps are repeated for different sized inserts.

5.2.3 Experiment to measure the temperature profile along the centerline

- Step 1.** The temperature sensor is suspended in the VT through the tube.
- Step 2.** Air is supplied at a pre-determined pressure and the system is left to achieve thermal stability (approx. 10 minutes).
- Step 3.** Temperatures (inlet and internal) are measured.
- Step 4.** VT is moved along the linear stage by a pre-determined distance and the temperatures are measured.
- Step 5.** Steps 3 & 4 are repeated till the entire length of the VT is covered.
- Step 6.** Steps 2 – 5 are repeated at a different supply pressure.

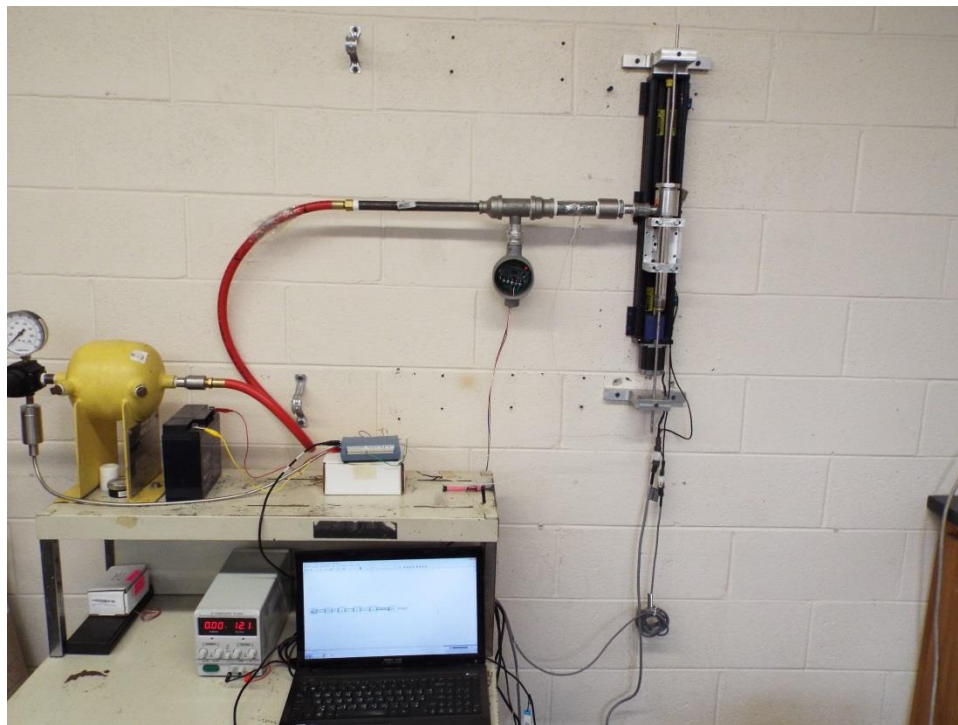
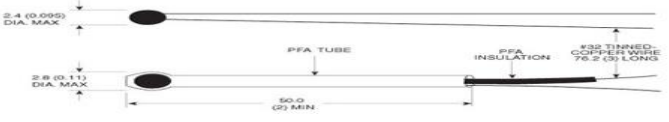
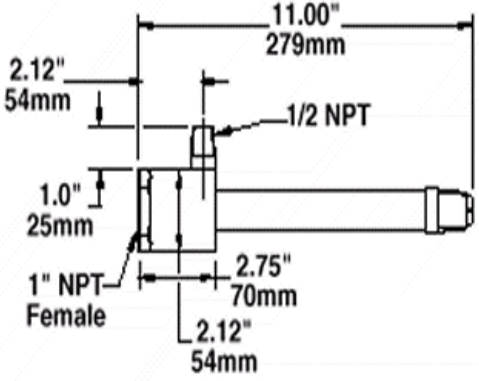
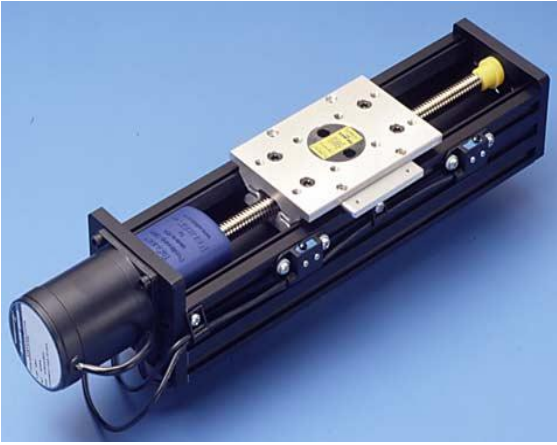


Figure 24. Setup for measuring centerline temperature profile.

5.3 Instrumentation

Following table gives details about the instruments used in the study.

<p>Thermistor (Omega – 44007)</p>	 <p style="text-align: center;">Figure 25. Thermistor</p>	<ul style="list-style-type: none"> • Interchangeability: ± 0.2 °C. • Maximum T: 150 °C. • Time constant, Max: 1 sec in well 																																																																																																																														
<p>Pressure Gauge (Ashcroft)</p>	 <p style="text-align: center;">Figure 26. Pressure Gauge</p>	<ul style="list-style-type: none"> • Range: Dual 0-100 psi & 0-700 kPa. • Dual: 3-1/2" • Pipe Size: 1/4" 																																																																																																																														
<p>Vortex Tube (Exair – 3499)</p>	 <p style="text-align: center;">Figure 27. Vortex Tube</p>	<table border="1" data-bbox="1154 1346 1560 1793"> <thead> <tr> <th colspan="8">Performance Data</th> </tr> <tr> <th rowspan="2">Pressure Supply</th> <th colspan="7">Cold Fraction %</th> </tr> <tr> <th>PSIG</th> <th>20</th> <th>30</th> <th>40</th> <th>50</th> <th>60</th> <th>70</th> <th>80</th> </tr> </thead> <tbody> <tr> <td rowspan="2">20</td> <td>**</td> <td>62</td> <td>60</td> <td>56</td> <td>51</td> <td>44</td> <td>36</td> <td>28</td> </tr> <tr> <td>**</td> <td>15</td> <td>25</td> <td>36</td> <td>50</td> <td>64</td> <td>83</td> <td>107</td> </tr> <tr> <td rowspan="2">40</td> <td>**</td> <td>88</td> <td>85</td> <td>80</td> <td>73</td> <td>63</td> <td>52</td> <td>38</td> </tr> <tr> <td>**</td> <td>21</td> <td>35</td> <td>52</td> <td>71</td> <td>92</td> <td>117</td> <td>147</td> </tr> <tr> <td rowspan="2">60</td> <td>**</td> <td>104</td> <td>100</td> <td>93</td> <td>84</td> <td>73</td> <td>60</td> <td>46</td> </tr> <tr> <td>**</td> <td>24</td> <td>40</td> <td>59</td> <td>80</td> <td>104</td> <td>132</td> <td>166</td> </tr> <tr> <td rowspan="2">80</td> <td>**</td> <td>115</td> <td>110</td> <td>102</td> <td>92</td> <td>80</td> <td>66</td> <td>50</td> </tr> <tr> <td>**</td> <td>25</td> <td>43</td> <td>63</td> <td>86</td> <td>113</td> <td>143</td> <td>180</td> </tr> <tr> <td rowspan="2">100</td> <td>**</td> <td>123</td> <td>118</td> <td>110</td> <td>100</td> <td>86</td> <td>71</td> <td>54</td> </tr> <tr> <td>**</td> <td>26</td> <td>45</td> <td>67</td> <td>90</td> <td>119</td> <td>151</td> <td>191</td> </tr> <tr> <td rowspan="2">120</td> <td>**</td> <td>129</td> <td>124</td> <td>116</td> <td>104</td> <td>91</td> <td>74</td> <td>55</td> </tr> <tr> <td>**</td> <td>26</td> <td>46</td> <td>69</td> <td>94</td> <td>123</td> <td>156</td> <td>195</td> </tr> </tbody> </table> <p>* Temperature drop of cold air, °F ** Temperature rise of hot air, °F</p>	Performance Data								Pressure Supply	Cold Fraction %							PSIG	20	30	40	50	60	70	80	20	**	62	60	56	51	44	36	28	**	15	25	36	50	64	83	107	40	**	88	85	80	73	63	52	38	**	21	35	52	71	92	117	147	60	**	104	100	93	84	73	60	46	**	24	40	59	80	104	132	166	80	**	115	110	102	92	80	66	50	**	25	43	63	86	113	143	180	100	**	123	118	110	100	86	71	54	**	26	45	67	90	119	151	191	120	**	129	124	116	104	91	74	55	**	26	46	69	94	123	156	195
Performance Data																																																																																																																																
Pressure Supply	Cold Fraction %																																																																																																																															
	PSIG	20	30	40	50	60	70	80																																																																																																																								
20	**	62	60	56	51	44	36	28																																																																																																																								
	**	15	25	36	50	64	83	107																																																																																																																								
40	**	88	85	80	73	63	52	38																																																																																																																								
	**	21	35	52	71	92	117	147																																																																																																																								
60	**	104	100	93	84	73	60	46																																																																																																																								
	**	24	40	59	80	104	132	166																																																																																																																								
80	**	115	110	102	92	80	66	50																																																																																																																								
	**	25	43	63	86	113	143	180																																																																																																																								
100	**	123	118	110	100	86	71	54																																																																																																																								
	**	26	45	67	90	119	151	191																																																																																																																								
120	**	129	124	116	104	91	74	55																																																																																																																								
	**	26	46	69	94	123	156	195																																																																																																																								

<p>Linear Stage (Velmex – MN10-0160- M02-21)</p>	 <p>Figure 28. Velmex Bislide Linear Stage</p>	<ul style="list-style-type: none"> • M: Cross Section. • N: Nut/Screw Drive. • 10: Design in Inch. • 0160: Travel. (16 inch) • M02: 2.00mm Advance/turn. • 21: NEMA 23 Mount & Limit Switches.
<p>Precision Turbine Flow Meters (Omega – 930 series)</p>	 <p>Figure 29. Precision Turbine Flow meter with signal conditioner.</p>	<ul style="list-style-type: none"> • Accuracy: $\pm 1.0\%$ of reading • Repeatability: $\pm 0.25\%$ • Body: 304/316 stainless steel • Rotor: 17-4 PH SS • Bearings: 440C stainless steel • Output: 30 mV p-p sinewave min.

**Signal
Amplifier
(Omega –
FLSC 64)**



Figure 30. Signal Amplifier

The FLSC-64 amplifies and conditions low-amplitude signals such as those developed by a magnetic pickup coil. The amplitude of the square wave output equals the input supply voltage of the FLSC-64. A sensitivity adjustment permits the FLSC-64 to discriminate between an input signal and noise. It can be directly mounted on the flow meter as seen in Figure . Frequency of the square wave generated by the flow meter will be proportional to the flow rate of air

**Stroboscope
(Genrad –
Strobotac
Type 1531)**



Figure 31. Stroboscope

- Calibration: Accurately calibrated flash rates to 25,000 per minute.
- Flash Rate (fpm): 110 to 25,000 in 3 ranges; speeds up to 250,000 rpm can be measured.
- Accuracy: 1% of reading after calibration on one range against 50-to-60 Hz line frequency

<p>Pressure Transducer (GP50 – 211)</p>	 <p>Figure 32. Pressure Transducer</p>	<ul style="list-style-type: none"> • Range: 0 -300 Psi. • Excitation voltage: 9.0 to 36 Vdc. • Output Signal: 0 to 5 Vdc • MOC: 17-4 PH SS. • Accuracy: $\pm 0.5\%$ FSO • Connection: 1/4"
<p>Data Acquisition Card (MCC DAQ – USB – 1208HS)</p>	 <p>Figure 33. Data Acquisition Card</p>	<ul style="list-style-type: none"> • 8 single-ended/4 differential analog inputs • 13-bit resolution • 1 MS/s sample rate • Single-ended ranges: ± 10 V, ± 5 V, ± 2.5 V or 0 to 10 V • Differential ranges: ± 20 V, ± 10 V, or ± 5 V • 16 digital I/O lines • Two 32-bit counters • One 32-bit PWM timer output • USB-bus powered

Table 1. Instrumentation

CHAPTER 6

REFERENCES

6.1 References for figures

- Figure 1. http://ethesis.nitrkl.ac.in/2069/1/final_thesis.pdf
- Figure 2. <http://www.exair.com/>
- Figure 3. https://www.youtube.com/watch?v=Q_y2FvH2DHE
- Figure 4. <http://www.scienceforums.net/topic/53028-ranque-hilsch-vortex-tube-and-golden-spiral/>
- Figure 18. http://www.omega.com/pptst/44000_THERMIS_ELEMENTS.html
- Figure 20. <http://www.exair.com/>
- Figure 21. <http://www.velmex.com/>
- Figure 22. <http://www.omega.com/pptst/FTB930.html>
- Figure 23. <http://www.omega.com/pptst/FLSC60.html>
- Figure 25. <http://www.gp50.com/product/model-111-211-311-industrial-grade-pressure-transmitter-automotive-testing/>
- Figure 26. <http://www.mccdaq.com/usb-data-acquisition/USB-1208HS.aspx>

6.2 References for literature review

- [1] G.J. Ranque, “Expériences sur la détente giratoire avec production simultanée d’un échappement d’air chaud et d’un échappement froid”, *J. Phys. Radium* 4 (1933) 112.
- [2] R. Hilsch, “The use of the expansion of gases in a centrifugal field as cooling process”, *Rev. Sci. Instrum.* 18 (2) (1947) 108.
- [3] Mahyar Kargaran, Mahmood Farzaneh-Gord, “An Experimental study on the effect of pressure inlet gas on a counter-flow vortex tube”, *Frontiers in Heat and Mass Transfer (FHMT)*, 4, 013007 (2013).
- [4] Nader Pourmahmoud, Masoud Rahimi, Seyyed Ehsan Rafiee, Amir Hassanzadeh, “A numerical simulation of the effect of inlet gas temperature on the energy separation in a vortex tube”, *Journal of Engineering Science and Technology* Vol. 9, No. 1 (2014) 81 – 96.
- [5] C.U. Linderstrom-Lang. “A model of gas separation in Ranque-Hilsch vortex tubes”. *Z. Naturforsch.*, 22(a):835–837, April 1967.
- [6] J. Marshall, “Effect of operating conditions, physical size and fluid characteristics on the gas separation performance of a Linderstrom-Lang vortex tube”. *Int. J. Heat Mass Transfer*, 20:227–231, 1977.

- [7] Rajarshi Kar, Oindrila Gupta, Mukunda Kumar Das, "Studies on the Effect of Feed Gas Temperature on Ranque-Hilsch Vortex Tube", International Journal of Scientific and Research Publications, Volume 2, Issue 11, November 2012, ISSN 2250-3153.
- [8] Orhan A., Baki Muzzafer, 2006, "An Experimental Study on the Design Parameters of a Counterflow Vortex Tube", *Energy* 31, 2763-2772.
- [9] Pourmahmoud, N, Rafiee, S.E, Rahimi M, and Hassanzadeh, A, "Numerical energy separation analysis on the commercial Ranque-Hilsch vortex tube on basis of application of different gases", *Scientia Iranica B*, 20(5), 1528-1537.
- [10] Sachin Nimbalkar, Michael R. Muller, "An experimental investigation of the Optimum geometry for the cold end orifice of a vortex tube", *Applied Thermal Engineering* 29 (2009) 509-514.
- [11] Pourmahmoud N, Bramo A R, "The effect of L/D ratio on the temperature Separation in the counterflow vortex tube", *IJRRAS* 6(1) January 2011.
- [12] Volkan Kirmaci, "Optimization of counter flow Ranque-Hilsch vortex tube performance using Taguchi method", *International Journal of Refrigeration*, vol 32; ppl487-1494 (2009).
- [13] Y.T, Wu, Y. Ding, Y.B. Ji, C.F. Ma, M.C. Ge, "Modification and experimental research on vortex tube:", *International Journal of Refrigeration*, 30 (2007) 1042-1049.
- [14] Pourmahmoud N, Esmaily R, Hassanzadeh A, "CFD investigation of vortex tube length as a designing criterion", *International Journal of Heat and Technology*, Vol.33, No.1, 2015.
- [15] Schultz-Grunow F 1951 "Turbulenter Wmnedurchgang im Zentrifugalfeld" *Forsch Ing. Wes.* 17 65-76.
- [16] Ahlborn, B., Keller, J.U., Staudt, R., Treitz, G., Rebhan, E. "Limits of temperature separation in a vortex tube", *J. Phys. D.: Appl. Phys.*, 27:480-488, 1994.
- [17] Kurosaka, M., Chu, J.Q. & Goodmann, J.R. "Ranque-Hilsch effect revisited: Temperature separation effect traced to orderly spinning waves or vortex whistle", *AIAA (82-0952) AIAA/ASME 3rd Joint Thermo-Physics of Fluids, Plasma and Heat Transfer Conference*, 1982.
- [18] Ahlborn B, Groves S, "Secondary flow in a vortex tube", *Fluid Dynamics Research* 21 (1997) 73-86.
- [19] R Liew, J C H Zeegers, J G M Kuerten and W R Michalek, "Temperature, Pressure and Velocity measurements on the Ranque-Hilsch Vortex Tube", 6th European Thermal Sciences Conference (Eurotherm 2012), *Journal of Physics: Conference Series* 395 (2012) 012066.
- [20] M.H. Saidi, M.R. Allaf Yazdi, "Exergy model of a vortex tube system with experimental results", *Energy* 24 (1999) 625-632.
- [21] Y. Xue and M. Arjomandi, "Thermodynamic analysis of the energy separation in a counter-flow vortec tubes", 19th Australian Fluid Mechanics Conference, 8-11 December 2014.
- [22] K. Stephen, S. Lin, M. Durst, F. Huang and D. Seher, "An investigation of energy separation in a vortex tube", *International Journal of Heat Mass Transfer*, Vol. 26(3), pp. 341-348, 1983.

- [23] Chang Hyun-Sohn, Chang-Soo Kim, Ui-Hyun Jung and B.H.L Lakshmana Gowda, “Experimental and Numerical studies in a vortex tube”, *Journal of Mechanical Science and Technology (KSME Int. J.)*, Vol. 20, No. 3, pp. 418-425, 2006.
- [24] Choi B.C and Riu. K.J., 1996, “An Experimental Study for Cold End Orifice of Vortex Tube”, *Transaction of the KSME B in Korea*, Vol.42, pp. 415-422.
- [25] S. Nimbalkar, Michael R. Muller, “Quantitative observations on multiple flow structures inside Ranque Hilsch vortex tube”,
<https://rucore.libraries.rutgers.edu/rutgers-lib/25863/pdf/1>.
- [26] Saidi M.H., Valipour M.S., “Experimental modeling of vortex tube refrigerator”, *Applied Thermal Engineering* 23 (2003) 1971-1980.
- [27] Khodorkov I.L., Poshernov N.V. and Zhidkov M.A., “The vortex tube – a universal device for heating, cooling, cleaning, and drying gases and separating gas mixtures”, *Chemical and Petroleum Engineering* 39 (7-8) (2003) 409-415.
- [28] Stanescu G, Cabral C., Santos M.C, “Experimental study on the vortex tube potential to increase air moisture removal and carrying capability”, 15th International Conference on Experimental Mechanics, 2931.
- [29] Saha D., Zeegers J.C.H, Kuerten J.G.M, “Condensation and droplet separation in Ranque-Hilsch vortex tube”, 13th International Conference on Multiphase Flow in Industrial Plants, Sestri Levante, Genova, Italy 2014.
- [30] Liew R., Michalek W. R., Zeegers J.C.H., Kuerten J.G.M., “Droplet Behavior in a Ranque-Hilsch vortex tube”, 13th European Turbulence Conference (ETC13), *Journal of Physics: Conference Series* 318 (2011) 052013.
- [31] Grönner J., “Successful experience with vortex tube technology at the EPE Cavity Storage of RWE Energy”, 23rd World Gas Conference, Amsterdam 2006.
- [32] <https://www.vortec.com/c-11-vortex-tubes.aspx>
- [33] <http://www.exair.com/>
- [34] T. Cockerill., Ranque-Hilsch vortex tube, Master thesis, University of Cambridge, 1995.